



Merfin: improved variant filtering, assembly evaluation and polishing via k -mer validation

Giulio Formenti^{1,2,3,8}✉, Arang Rhie^{4,8}✉, Brian P. Walenz⁴, Françoise Thibaud-Nissen⁵, Kishwar Shafin⁶, Sergey Koren⁴, Eugene W. Myers⁷, Erich D. Jarvis^{1,2,3} and Adam M. Phillippy⁴

Variant calling has been widely used for genotyping and for improving the consensus accuracy of long-read assemblies. Variant calls are commonly hard-filtered with user-defined cutoffs. However, it is impossible to define a single set of optimal cutoffs, as the calls heavily depend on the quality of the reads, the variant caller of choice and the quality of the unpolished assembly. Here, we introduce Merfin, a k -mer based variant-filtering algorithm for improved accuracy in genotyping and genome assembly polishing. Merfin evaluates each variant based on the expected k -mer multiplicity in the reads, independently of the quality of the read alignment and variant caller's internal score. Merfin increased the precision of genotyped calls in several benchmarks, improved consensus accuracy and reduced frameshift errors when applied to human and nonhuman assemblies built from Pacific Biosciences HiFi and continuous long reads or Oxford Nanopore reads, including the first complete human genome. Moreover, we introduce assembly quality and completeness metrics that account for the expected genomic copy numbers.

Accurate variant calling has been a challenge in medical genomics, especially to achieve both high recall and precision in hard-to-measure regions¹. The advent of next-generation sequencing (NGS) and long-read sequencing technologies streamlined variant calling², which typically includes (1) aligning all reads to a reference genome; (2) calling variants from the alignment; and (3) filtering to remove false positives. The final outcome relies heavily on the precision of this multistep procedure, which depends on (1) the quality of the read set; (2) the precision of the read-mapping algorithm; and (3) the precision of the variant caller in generating reliable calls³. To remove false positives, variant calls are often hard-filtered using heuristics, such as requiring a minimum coverage support, genotype quality or other internal quality scores². However, no universally applicable cutoffs exist as they vary depending on the sequencing technology used. Therefore, the accuracy of a variant corresponds to the theoretical limit of the algorithms and the cutoffs employed, and not to the theoretical limit given the quality of the raw data.

In parallel, new sequencing technologies greatly expanded our genome assembly toolkit. While the short-reads stumbled resolving repetitive regions⁴, long reads have considerably improved the contiguity of genome assemblies⁵. However, reduced consensus accuracy (hereby noted as QV) has been progressively acknowledged due to the lower base-calling accuracy in long reads, at least until the more recent Pacific Biosciences (PacBio) high-fidelity (HiFi) reads became available⁶. Still, lower QV remains even in HiFi reads for simple repeat sequences, particularly homopolymers^{7,8}. Reduced QV has detrimental impacts on many downstream analyses, such as gene annotation, which requires an accurate consensus to predict the correct coding sequence⁷. To mitigate this issue, 'polishing' tools have been developed, such as Pilon, Arrow, Racon and Medaka^{9–11}, and established variant-calling tools such as GATK, Freebayes and

DeepVariant^{12–14} have been repurposed to detect errors and find candidate corrections. Unlike resequencing-based methods, the assembly from the same genome is used as a reference for polishing, and thus all homozygous variants suggest corrections to be made. Once corrections are collected, the consensus can be updated using tools such as Bcftools¹⁵. The process is usually repeated with different read sets (such as long and short reads), until the QV reaches a set standard.

QV has been historically measured from the variant-calling process as described above; however, bearing biases caused from mapping or variant calling. In our previous work, we presented Merqury¹⁶, an alignment-free approach to estimate base-level QV using k -mers (genomic substrings of length k). In Merqury, k -mers found only in the assembly and not in the reads are considered as errors, disregarding the expected copy number. As a result, overly represented k -mers from sequence expansion (false duplications) in the assembly are considered as correct bases. Merqury also presents a completeness metric from the portion of k -mers found in the assembly from a given reliable k -mer set in reads; however, this k -mer completeness metric does not account for the k -mer multiplicity in the reads, limiting the scope in the non-repetitive k -mer space. As a result, any two assemblies with identical distinct k -mers will score the same completeness metric, regardless of one having higher sequence collapses or expansions.

Ideally, the sequence of an error-free and complete genome assembly is in perfect agreement with the sequence data, assuming that genomic DNA is randomly sampled with negligible sequencing biases. Therefore, any changes introduced during polishing should improve the assembly-read agreement. This principle has been widely used to visually evaluate genome assembly copy-number spectrum (such as spectra-cn analysis^{16,17}) and more recently, used to detect errors and improve read alignment^{18–20}. However, none

¹Vertebrate Genome Laboratory, The Rockefeller University, New York, NY, USA. ²Laboratory of Neurogenetics of Language, The Rockefeller University, New York, NY, USA. ³Howard Hughes Medical Institute, Chevy Chase, MD, USA. ⁴Genome Informatics Section, Computational and Statistical Genomics Branch, National Human Genome Research Institute, National Institutes of Health, Bethesda, MD, USA. ⁵National Center for Biotechnology Information, National Library of Medicine, National Institutes of Health, Bethesda, MD, USA. ⁶UC Santa Cruz Genomics Institute, Santa Cruz, CA, USA. ⁷Max Planck Institute of Molecular Cell Biology and Genetics, Dresden, Germany. ⁸These authors contributed equally: Giulio Formenti, Arang Rhie. ✉e-mail: gformenti@mail.rockefeller.edu; arang.rhie@nih.gov

of the evaluation metrics or polishing methods has fully utilized assembly-read agreement.

Here, we introduce a k -mer-based filtering approach that is applicable to genomic variant calls, which achieved higher F1 scores compared to parameter-based hard-filtering methods. Next, we propose revised QV and completeness scores that account for the expected sequence copy number given a k -mer frequency, driven by our refined K^* definition²¹ for genome assembly evaluation. Our K^* enables the detection of collapses and expansions and substantially improves the QV when used to filter variants for polishing. We applied this approach to evaluate the most complete HiFi-based assembly of CHM13 (refs. 22–25), simultaneously released by the Telomere-to-Telomere (T2T) Consortium²². Next, we polished an Oxford Nanopore-based trio assembly from the Human Pangenome Reference Project (HPRC)²⁶ and three continuous long read (CLR)-based haploid and pseudo-haploid assemblies (fish, reptile and bird) generated by the Vertebrate Genomes Project (VGP)⁵, all resulting in substantially higher consensus accuracy and annotation quality. This approach is implemented as Merfin (a k -mer-based finishing tool) and is publicly available. Merfin requires k -mers from highly accurate reads (e.g. Illumina) that reflect the k -mer frequency in the genome.

Results

Variant-call filtering for higher precision. A reference genome with its sequence replaced at all alternate variant calls can be considered a ‘consensus’ sequence and evaluated with k -mers. Unlike using a *de novo* assembled genome of the same individual as a reference, natural biological differences between the sequenced individual and the reference genome or the incomplete state of the reference (missing a segmental duplication) imposes challenges to reliably call variants. Nevertheless, it is possible to construct consensus paths from a variant or series of variants within k base pairs (bp) and confirm its validity. We can score each path by the number of k -mers never found in the reads (error k -mer) and choose the best path to contain minimal error k -mers (Fig. 1a and Extended Data Fig. 1a; ‘filter’ mode).

To test the validity of this filtering approach, we benchmarked against unfiltered (default) and hard-filtered variant calls submitted to precisionFDA challenge II, HG002 (ref. 1). The variants were called from Illumina reads or from multiple platforms (Illumina, PacBio HiFi and ONT) using GRCh38 as the reference with GATK HaplotypeCaller. Hard-filtering was performed using the variant caller’s internal scores such as PASS, QD, MQ and QUAL. When comparing precision, recall and F1 score (harmonic mean of precision and recall) on a truth set of Chr. 20 (ref. 27), Merfin always achieved higher precision with minimal loss in recall on both default and hard-filtered sets (Fig. 1b). The hard-filtered set had higher precision, with the price of losing more true positives, resulting in a lower F1 score when compared to the default set. Merfin was able to remove additional false positives on the hard-filtered set. True-positive variants used in this analysis, ranging from 48-bp deletions to 47-bp insertions, were all recovered by Merfin.

Assembly evaluation. When a reference genome is constructed from the same individual, the k -mer multiplicity seen in the reads is expected to match the reference. This property can be used for evaluating *de novo* assembled genomes. Here, we introduce our revised K^* , which identifies potentially collapsed and expanded regions in an assembly and quantitative metrics for representing assembly copy-number concordance and completeness.

Identifying collapsed and expanded regions. The K^* metric was defined previously to detect identical collapsed repeats on each k -mer in the assembly²¹. The method proposed $K^* = K_R / K_C$, where K_R is the frequency of a k -mer found in the reads; and K_C is the

frequency of a k -mer across the entire consensus sequence of the assembly. In regions with no collapsed repeats, K^* will be equal to c , the average coverage of sequencing reads. Here we revised the K^* such that it evaluates both collapses and expansions. We propose $K^* = (K_r - K_c) / \min(K_r, K_c)$, where K_r is the expected copy number inferred from the reads (Fig. 1c). For a perfect genome assembly and an unbiased read set, K^* is normally distributed with mean 0 and deviations from the mean reflect natural variation in the Poisson sampling process (Fig. 1d). Conversely, any large deviation from the normal distribution can be interpreted either as a bias in the assembly (an assembly error) or a bias in the read set. Specifically, a positive K^* implies that the assembly contains fewer copies of k -mers than suggested by the read set (collapsed), whereas a negative K^* implies more copies in the assembly than suggested by the read set (expanded).

The K_r can be obtained by rounding to the nearest integer, $\lfloor K_r / c \rfloor$, where c is the haploid (one-copy) peak of the k -mer distribution of the reads. Here we assume that rounding K_r is sufficient to account for the s.d. associated with the Poisson process underlying read generation. While this is true in the case of a perfectly sampled sequencing set, the validity of this generalization is challenged in the presence of sampling bias, systematic error in the reads and variable degrees of heterozygosity that results in different likelihoods of specific copy numbers. To account for this uncertainty and improve the accuracy of the results, we modified Genomescope2 (ref. 28) to probabilistically infer K_r for each K_r , using the observed k -mer count distribution in the read set. If supplied, Merfin will use these probabilities for $K_r \leq 4$. (Fig. 1e).

QV* estimation. An average genome-wide QV accounting for excessive copy numbers (hereby defined as QV*) can be obtained using $\sum K_C - K_r$ as errors when $K_C > K_r$ for all positions in the assembly (Fig. 1f and Extended Data Fig. 1b; ‘hist’ mode). These excessive and error k -mers can be generalized as ‘errors’ in Phred-scale QV, as in Merqury¹⁶ or YAK²⁹.

Assembly completeness. The sum of $K_r - K_C$ (over all positions where $K_r > K_C$) expresses absent k -mers that should be present in the assembly and can be directly translated into a measure of assembly completeness as $1 - \sum (K_r - K_C) / K_r$ (Fig. 1f). Notably, contrary to other measures of assembly completeness based on a subset of the k -mers (such as relying only on the occurrence of distinct k -mers as in Merqury¹⁶), Merfin uses all k -mers, including their frequency and computes the fraction of the expected total number of k -mers (Extended Data Fig. 1b; ‘completeness’ mode).

Sequence polishing. The K^* becomes particularly useful in polishing. Increased QV is achievable through a dedicated polishing tool or via corrections identified by a standard variant-calling method. Even when using polishing tools, generating a set of potential corrections in variant-call format (VCF) allows finer control over the outcome and can be assessed with Merfin. In Merfin, the impact of each correction or combination of corrections are assessed from the given correction candidates by comparing the change in K^* metrics (Fig. 1a,c and Extended Data Fig. 1a; ‘polish’ mode). In addition to the error k -mers collected in each predicted consensus path, we compute the consequent k -mer frequency change and choose the correction only when it improves the assembly-read agreement. For example, when a suggestive correction (replacing AT with A as shown in Fig. 1a) introduces more error k -mers, it should not be used for polishing. Even when no error k -mers are introduced, K^* theoretically informs whether a path improves the assembly-read agreement in polishing. The current implementation evaluates each path independently and thus only a local optimum is guaranteed. Variants within distance k are considered in all combinations, allowing

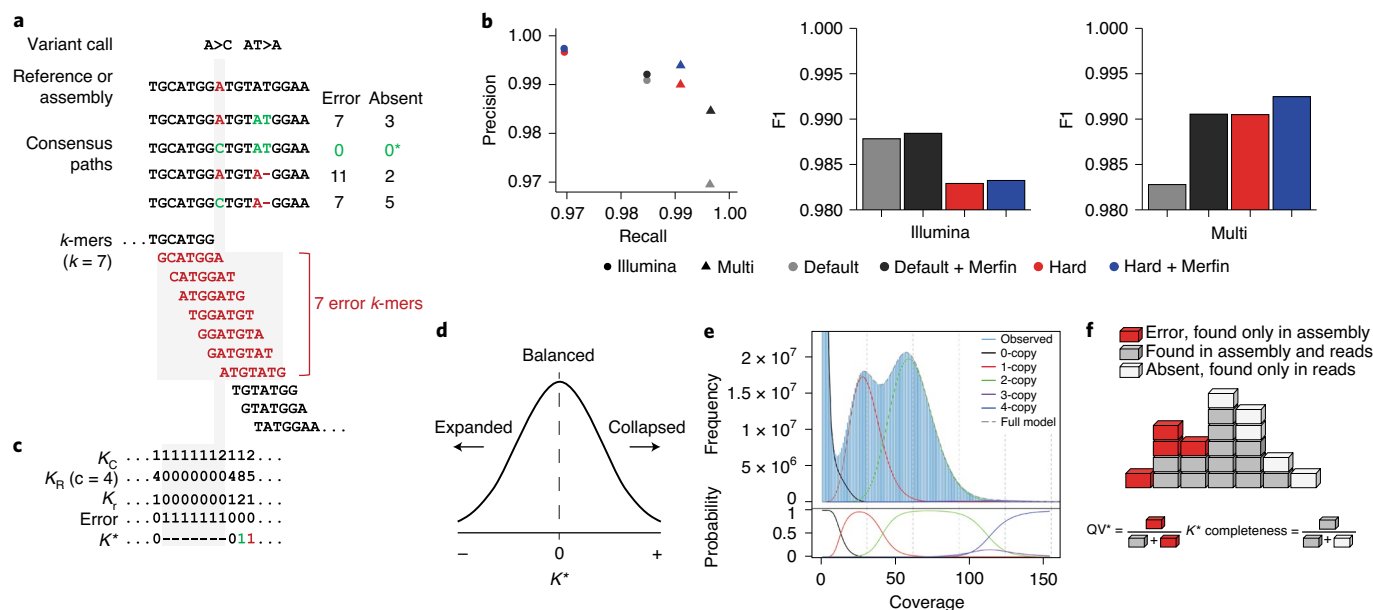


Fig. 1 | Algorithms and results used in Merfin. a, Two variant calls and their potential consensus paths. The bases and k -mers in red are errors not found in the reads. The path with A > C has no error k -mers and gets chosen for genotyping. For polishing, the average K^* is computed in addition to the missing k -mers using the predicted absent k -mers (*). **b**, Precision, recall and F1 score from a benchmark on HG002 genotyping. Merfin always achieves higher precision and F1 scores compared to the hard-filtered approach with almost no loss in recall. Default, no filtering; red, hard-filtering on default. **c**, K -mer frequency found in the consensus sequence (K_C), reads (K_R) with average coverage at four, expected copy number based on the corrected k -mer frequency ($K_f = K_R / c$) and K^* . Positive and negative K^* values are colored in green and red. The highlighted region (gray) shows the same k -mers and values used to compute K^* as affected by the A base in the reference. If two alternatives bear the same number of missing k -mers, the alternative with the K^* closest to zero is chosen. **d**, K^* distribution. K^* values deviated from 0 indicate collapsed (+) or expanded (-) k -mers in the assembly. **e**, Genomescope2 k -mer frequency histogram with theoretical k -multiplicity curves (top) and probabilities (bottom) for zero, one, two, three and four-copy k -mers, generated using the `-fitted_hist` option. Note that the three-copy peak is fully contained in the two- and four-copy peaks. **f**, Diagram for estimating QV^* and completeness from k -mers. Each k -mer is a block colored by its state of presence. In the block tower, each column represents the identical k -mer with its state colored by its presence in the assembly, reads or in both. Note the QV^* and K^* completeness use all k -mers, including their frequency.

Merfin to filter variant calls close to each other. This approach is fully independent of the raw dataset employed. For instance, the assembly could be generated using long reads and the calls evaluated using either short or long reads or both, taking advantage of the strengths of each sequencing platform, making accurate orthogonal validation possible, ultimately maximizing the assembly-read agreement.

Evaluating a complete human genome: T2T-CHM13. The CHM13hTERT (CHM13) cell line originates from a complete hydatidiform mole (46, XX), where both haplotypes are nearly identical³⁰. This cell line was used to generate the most complete high-quality human reference to date, resolving all centromeric and telomeric repeats and all segmental duplications and satellite arrays^{22,23}. Notably, T2T-CHM13v0.9 was polished from a variety of variant calls, filtered with an earlier version of Merfin, which improved the consensus accuracy of the final assembly²⁵. We further evaluated candidate assemblies to identify collapses and expansions using Merfin using k -mers from HiFi and Illumina reads. We found that the T2T-CHM13v1.0 assembly shows a remarkable agreement with the raw data, with only a few regions having K^* largely different from 0, coinciding with satellite repeats (Fig. 2a). Rather than being assembly errors, these disagreements were associated with context-dependent augmentation or depletion in HiFi and GC bias in Illumina^{22,25}. In HiFi, the sequencing coverage depends on sequence content²². Illumina has a similar dependence in GC context, introducing biases during library preparation, but not necessarily in the same direction seen in HiFi. Indeed, K^* derived from HiFi and Illumina k -mers

showed opposite behavior in some regions, e.g. the HSat3 of chromosome 9 (Fig. 2b). These effects were observed only on the highly repetitive regions of the genome.

Compared to a less-complete and less-accurate preliminary assembly, T2T-CHM13v0.7 (ref. ³¹), T2T-CHM13v1.0 had a higher agreement of the assembly with the k -mers derived from HiFi (Fig. 2c) and Illumina reads (Extended Data Fig. 2). We found a general agreement in K^* between HiFi and Illumina PCR-free k -mers, including regions with sequencing bias common to the two technologies (Extended Data Fig. 3). In other cases, the direct comparison of the K^* computed from the two technologies highlighted technology-specific sequencing biases (Fig. 2a,d). Particularly, genome-wide comparison of the K^* computed using HiFi versus Illumina k -mers on the v1.0 assembly show substantial agreement between the assembly and the raw reads (Fig. 2d; coordinates 0, 0). The only k -mers consistently seen as under-represented in both technologies (Fig. 2d; top right quadrant) were mostly contributed from the un-assembled ribosomal DNAs (rDNAs) later resolved in v1.1 (ref. ²²). At base resolution, the K^* could distinguish regions with accurate consensus from bp errors, small and large indels, heterozygous sites and collapsed/expanded regions (Extended Data Fig. 4a,b).

Both QV and QV^* measured with Merqury and Merfin improved from v0.7 to v0.9 (ref. ²⁵), which involved a complete reassembly of the genome using HiFi reads and patches from v0.7 at GA-rich sequence dropouts in the HiFi reads (Supplementary Table 1). Merqury QV improved from v0.7 to v0.9, due to the dramatic decrease in error k -mers, however the Merfin QV^* only marginally increased as the number of error k -mers is small compared to

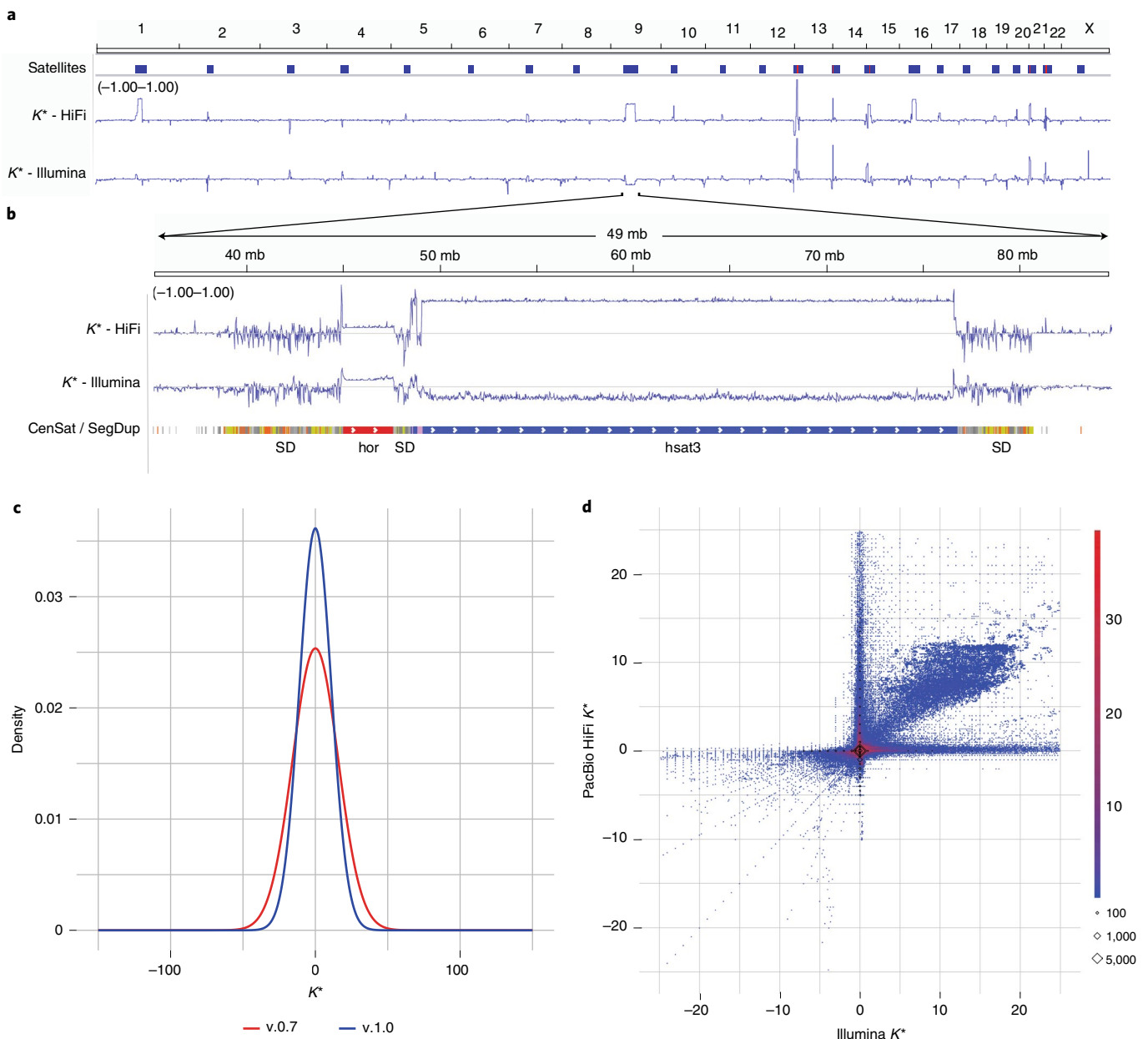


Fig. 2 | CHM13 evaluation and polishing. **a**, Genome-wide K^* for the T2T-CHM13 assembly v1.0. Satellites are associated with repeat- and technology-specific biases. Yet to be resolved rDNA arrays (red) are highlighted by positive K^* . **b**, Highlight of the centromeric satellite repeats⁴⁵ and segmental duplications (SDs)²³ (orange indicates most similar, yellow less and gray least) on chromosome 9. hor, higher-order repeat. **c**, Genome-wide density distribution of the K^* using HiFi k -mers. When the assembly is in agreement with the raw data, the K^* is normally distributed with mean 0 and the smaller the s.d. the higher the agreement. T2T-CHM13v1.0 shows a less-dispersed distribution of the K^* compared to a less-complete v0.7 assembly. **d**, Genome-wide comparison of the K^* computed using HiFi versus Illumina k -mers on the v1.0 assembly. Agreement between the assembly and the raw reads supported by the two technologies is found around (0, 0). The quadrant highlights where both HiFi versus Illumina technologies suggest the presence of underrepresented k -mers that were largely contributed from the un-assembled rDNAs later resolved in v1.1 (ref. 22) (top right); the quadrant highlights where both technologies suggest the presence of overrepresented k -mers (with perfect agreement found on the diagonals) (bottom left). The axes correspond to regions of substantial disagreement between the two technologies. Diamonds indicate k -mers missing from one (x or y axis) or both (0, 0) technologies.

the number of overly represented k -mers, likely due to sequencing biases. We argue that QV^* may still be a more reliable metric, because it accounts for all expected k -mer copy numbers, reflecting the full extent of genome representation. QV^* is also only marginally influenced by the coverage, as shown by a titration experiment (Extended Data Fig. 5 and Supplementary Table 2).

Polishing a completely phased assembly: HG002. The need for polishing is particularly evident in genome assemblies generated

using noisy long reads. Therefore, we tested Merfin's variant-calling filtering algorithm on an Oxford Nanopore-based assembly of human HG002 trio data generated by the HPRC using Flye^{32,33,26}. We benchmarked Merfin on Medaka, by comparing polishing outcomes from Medaka with or without filtering with Merfin. In a trio setting, the optimal approach is to polish each parental assembly separately, by aligning the binned reads and performing variant calling^{5,34}. This will reduce the introduction of haplotype switches. However, our k -mer-based evaluation of the corrections is best

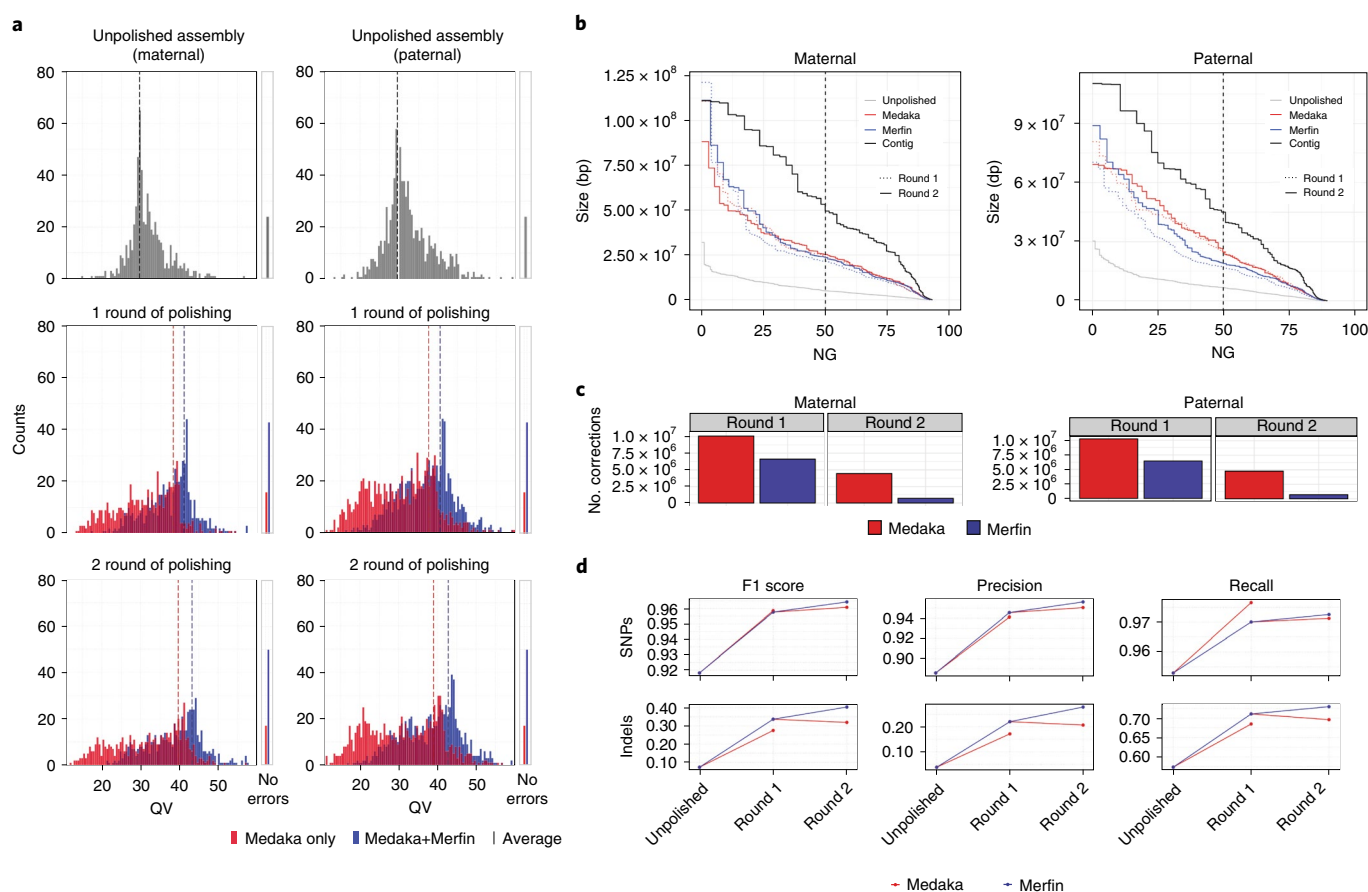


Fig. 3 | HG002 human trio polishing and evaluation. **a**, Distribution of QV scores as measured by Merqury for maternal and paternal contigs polished only with Medaka or with variants generated by Medaka filtered with Merfin, from the experiment (test 4, Supplementary Table 3) using latest basecaller (Guppy 4.2.2) and highest coverage ($\sim 50\times$). The first panel represents the unpolished contigs, the mid panel the first round of Medaka polishing and filtering and the last panel the second round applied to the Merfin results from the previous round. The number of contigs without evidence of errors as judged by Merqury QV are reported (right). **b**, Size of the haplotype blocks before and after polishing with or without Merfin for both the maternal and paternal assemblies. First round of polishing is represented by the dotted lines. NG, Size of the largest contig (or block) Y where contigs (blocks) $\geq Y$ cover $X\%$ of the estimated genome size. **c**, Number of variants generated by Medaka for polishing and remaining variants after Merfin filtering for both the maternal and paternal assemblies. **d**, Assembly-based HG002 small-variant-calling performance of Merfin versus regular Medaka against the GIAB truth set. Variants from the assembly are derived against GRCh38 using dipcall. SNP, single-nucleotide polymorphism.

performed on a combined assembly so that it faithfully represents the expected copy-number of each k -mer given the read set.

We first called variants separately from the binned reads used in the assembly with Medaka and then combined the variant calls and the parental assemblies for the Merfin variant-filtering step. K -mers used in Merfin were computed from Illumina sequencing reads. We conducted five different experiments using read sets that differ in coverage, the version of the Guppy basecaller and read length cutoff (Supplementary Table 3). Two rounds of polishing were conducted in all experiments, with the second round performed on the consensus from the first round generated with the additional Merfin step. Overall, in all experiments we observed comparable improvements in base-calling accuracy as measured by Merqury QV when Merfin filtering was applied (Supplementary Table 3). This increase reflected a dramatic positive shift in the QV distribution of individual contigs, with most low-quality contigs being rescued by Merfin and a sharp increase in the number of contigs found without errors, leading to a final Q43.2 and Q42.8 for maternal and paternal haplotypes, respectively (Fig. 3a). In the second round of polishing, the QV ceased to improve or even decreased when Merfin was not applied (Fig. 3a and Supplementary Table 3), suggesting that the best trade-off between errors corrected and

introduced in the assembly was already reached in the first round. In contrast, QV continued to increase relative to the first round with Merfin. Haplotype blocks as defined by Merqury increased in a comparable if not better way when using Merfin (Fig. 3b), while haplotypes remained fully phased (Extended Data Fig. 6). Notably, the results with Merfin were achieved by introducing only a fraction of the variants proposed by Medaka, making this approach more conservative than regular polishing (Fig. 3c).

We further validated the HG002 unpolished and polished assembly by aligning each haplotype assembly to GRCh38 and deriving small variants. When benchmarked against the Genome in a Bottle (GIAB) v4.2.1 truth set²⁷, the results show that using Merfin we get a better F1 score, particularly at indels (Fig. 3d and Supplementary Table 4)^{27,35,36}.

Evaluation, polishing and annotation of pseudo-haploid assemblies. We next applied Merfin to the polishing steps of the VGP-assembly pipeline⁵ (Extended Data Fig. 7) on pseudo-haploid assemblies from three species (flier cichlid, *Archocentrus centrarchus*, fArcCen1; Goode's desert tortoise, *Gopherus evgoodei*, rGopEvg1; and zebra finch, *Taeniopygia guttata*, bTaeGut1). Using PacBio CLR and 10X Genomics linked reads for polishing,

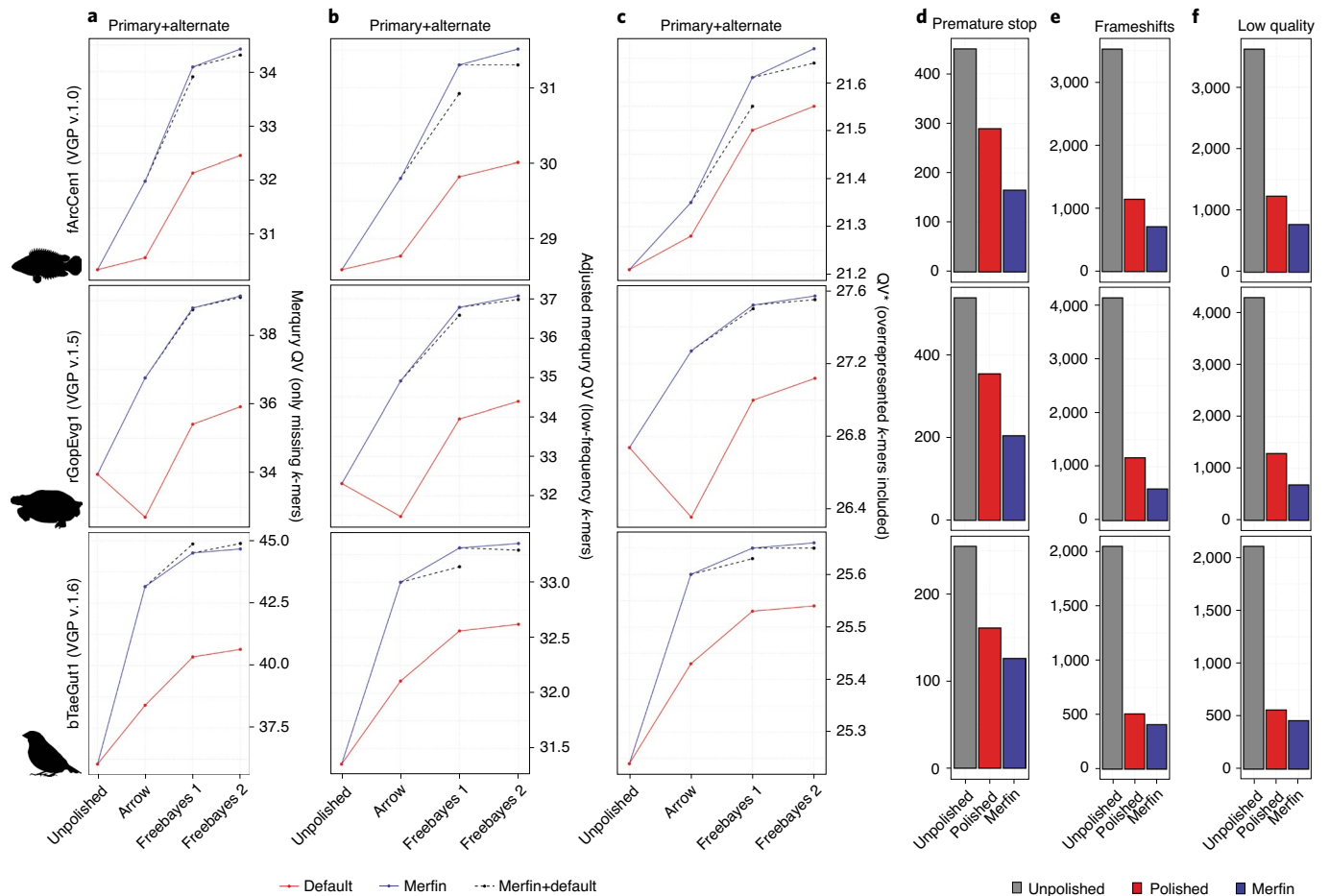


Fig. 4 | Polishing and evaluation of VGP pseudo-haploid assemblies. **a–c**, Polishing results of primary and alternate assemblies for the flier cichlid (fArcCen1), the Goode’s desert tortoise (rGopEvg1) and the zebra finch (bTaeGut1) using the VGP pipeline. Graphed are the unpolished QV values and the Merquy QV that accounts only for missing k -mers (**a**), the Merquy QV corrected using Merfin models for zero-copy k -mers (**b**) and QV* that also accounts for overrepresented k -mers (**c**). **d–f**, the general QV increase was reflected in the quality of the gene annotation, with consistent reduction in the number of genes affected by premature stop codons (**d**), frameshifts errors (**e**) and low-quality protein-coding gene predictions (**f**).

we observed a general improvement in QV as measured by Merquy (Fig. 4a and Supplementary Table 5). The largest improvement was observed in the first round of the Arrow polishing step using CLR. Arrow can replace low-quality sequences with patch sequences generated *de novo* from the reads that align to the region, independent of the original reference quality. We observed low coverage sequencing biases (homopolymer shortening) and mosaic haplotypes in the generated patches, leading to cases of lower QV in the polished assembly (Fig. 4a; rGopEvg1). Merfin rescued the QV decrease or improved the QV in all cases. The variant length range (–453:2,242) was not compromised after Merfin (–453:1,618) and many of the variants well above 50 bp were retained by Merfin (Supplementary Table 6), supporting the notion that if the quality of the consensus sequence is sufficient, large calls will not be negatively impacted.

In the subsequent polishing steps performed using Freebayes, the benefit of running Merfin to filter the variant set was less pronounced but still present (Fig. 4a; dashed lines). This was true in all cases except for the zebra finch, where the default pipeline performed marginally better. However, when considering low-frequency k -mers as errors from the probability model in Merfin, the QV as well as QV* increased in all cases (adjusted QV and QV*; Fig. 4b,c and Supplementary Table 5). Merquy QV counts all k -mers never seen in the reads as errors, whereas the adjusted QV additionally counts low-frequency k -mers based on the k -mer frequency

spectrum as errors. The QV* further includes overrepresented k -mers as errors, therefore capturing not only base accuracy errors, but also false duplications, expressing the uncertainty associated with any particular base given the support from the raw reads.

Most long-read assemblers generate locally phased haplotypes (such as Falcon-Unzip³⁷) and it is therefore important that the polishing does not introduce haplotype switches. To test whether the increase in QV from Merfin was due to introducing haplotype switches, we tested a zebra finch (*T. guttata*, bTaeGut2) pseudo-haploid assembly for which parental sequence information is available to evaluate, using parent-specific k -mers, the size of haplotype blocks and the number of haplotype switches⁵. When Merfin was applied to filter variants generated by Freebayes on the Longranger alignments of the 10X reads in the zebra finch pseudo-haploid setting, we noticed an increase in the number of haplotype switches as measured with Merquy (Supplementary Table 7). We realized that this was due to many heterozygous variants being called by Freebayes, when individual reads were mapped to collapsed regions or preferentially to the more-accurate primary assembly⁵. The missing true heterozygous k -mers in the collapsed or lower quality regions were recovered by the heterozygous variant call and thus preferred by Merfin. Further, even in almost complete pseudo-haploid assemblies, short reads can be easily mismapped, leading to spurious heterozygous calls. To overcome this issue,

we decided to remove all heterozygous variants before applying Merfin. This substantially prevented haplotype switches (Extended Data Fig. 8), without affecting the QV increase (Supplementary Table 7). In conclusion, we suggest removing all heterozygous variants before using Merfin as the best practice for polishing pseudo-haploid and haploid assemblies.

In addition, we validated our results using gene annotations, which are sensitive to consensus accuracy error and particularly to frameshift errors caused by indel errors. We performed *de novo* gene annotation using the RefSeq³⁸ gene annotation pipeline (Gnomon)³⁹ on the VGP assemblies polished with the conventional VGP pipeline (v1.6) and compared against assemblies where Merfin was applied at every polishing step. In Gnomon, if a protein alignment supports a predicted model with an indel introducing frameshift or premature stop codons, the model is labeled as 'low quality' and a base is added or removed from the predicted model to compensate for the indel in the genome. If more than one in ten coding genes in an assembly require corrections, the assembly is excluded from RefSeq. Based on information provided by the submitters, almost all rejected assemblies used ONT or PacBio CLR reads.

Again, Merfin substantially reduced the number of genes affected by frameshifts, validating QV and QV* results (Fig. 4d–f, Supplementary Table 8 and an example in Extended Data Fig. 9). Premature stop codons were significantly reduced with respect to the default polishing in all cases (Fig. 4d), with 42.9%, 42% and 21.7% reduction in fArcCen1, rGopEvg1 and bTaeGut1, respectively. Ultimately, 1% or less of genes had code breaks in all cases when using Merfin. Frameshifts were also positively affected (Fig. 4e), with 38%, 49.6% and 19.5% reductions in fArcCen1, rGopEvg1 and bTaeGut1, respectively. Less than 3% of genes had frameshifts in all cases when using Merfin. Similarly, the number of protein-coding gene predictions labeled as 'low quality' were reduced (Fig. 4f). From these results, Merfin has been included in the VGP pipeline (v1.7).

Consistent with the variant filtering for genotyping, the improvements in QV with Merfin superseded any hard-filtering attempt using variant-call quality score (QUAL) cutoffs at the Arrow polishing step (Fig. 5a–c and Supplementary Table 9). For the primary assembly, QV* estimates were consistently higher than the best results attainable by hard filtering (fArcCen1, Q32.5 versus Q31.9 at $QUAL \geq 18$; rGopEvg1, Q38.7 versus Q36.7 at $QUAL \geq 21$; bTaeGut1, Q44.4 versus Q42.4 at $QUAL \geq 21$). The best QUAL cutoff was not necessarily consistent between species, indicating that a single cutoff cannot produce the best outcome in all cases. The alternate assembly (alternate haplotype) behaved similarly to the primary assembly, again with Merfin always performing best (fArcCen1, Q31.6 versus Q31.1 at $QUAL \geq 23$; rGopEvg1, Q35.2 versus Q34.2 at $QUAL \geq 26$; bTaeGut1, Q42.0 versus Q40.6 at $QUAL \geq 23$). However, it notably differed in best QUAL cutoff values to maximize QV. At increased QUAL cutoffs, both genuine and erroneous corrections are filtered out. Thus, hard-filtering cutoffs perform best when the number of errors corrected exceeds the number of errors introduced at maximum. In contrast, variants selected by Merfin had a wide range of quality scores, with the majority containing higher quality scores and yet including many below 25 (Fig. 5d–f). Notably, a significant fraction of variants with the highest quality score assigned were introducing error *k*-mers and thus were rejected by Merfin. Potentially, accumulated sequencing biases in long reads could lead to erroneous variant calls but these can be filtered with more-accurate *k*-mers from short reads. No hard-filtering methods were able to achieve QV improvements in polishing as observed with Merfin.

Effect of *k*-size and computational requirements. The minimum size of *k* can be determined by a given genome size and a tolerable *k*-mer collision rate⁴⁰. This has been adapted in Merquy¹⁶ and used

for *k*-mer-based assembly evaluation. In brief, under a maximum allowed collision rate of 0.5%, $k=21$ is suggested as the minimum length of *k* for genomes of size typically found in vertebrate species (1.2–4 Gb), including human and is used throughout our benchmarks. In theory, a larger *k* size could result in more-accurate filtering variants with the cost of *k*-mer coverage drop and increased computational burden. We tested whether using $k=31$ provides a better F1 score over $k=21$ on the variant-filtering GIAB benchmark and found that it provided a marginal improvement in the F1 scores (0.04%; Supplementary Table 10) at the cost of using 1.5-times more memory and 1.6 to 2.6-times more computation. As a large fraction of the read *k*-mers occur exactly once in the reads (72–89% of all distinct *k*-mers), we tested how excluding these would affect the performance of Merfin. Excluding unique *k*-mers in the filtering slightly increased the F1 score (0.01% to 0.03%) compared to using the entire *k*-mer set, by removing additional false-positive calls. Memory requirement substantially reduced from 122.6 GB to 49.2 GB for loading *k*-mers obtained from ~60× Illumina reads and 68 GB to 24.3 GB for loading ~25× Illumina reads along with reduced CPU hours (Supplementary Tables 10–12). As the filtering, evaluation and polishing results at different *k*-size or filtering were nearly identical, we recommend avoiding using larger *k* and excluding all unique *k*-mers before applying Merfin to maximize results with minimal computational burden.

Discussion

We described and demonstrated Merfin, a *k*-mer-based tool to evaluate and filter variant calls for improved genotyping accuracy and polishing. Notably, while adding only a modest runtime to variant calling, Merfin allows an innovative alignment-free evaluation and filtering of variants (VCF) generated from any dataset or variant-calling method. Merfin successfully removes false-positive calls, superseding any hard-filter-based cutoff for both genotyping and polishing. Contrary to the plateau effect usually observed in traditional polishing, our approach is a monotonic function, predicted to improve consensus accuracy until no more useful variants are produced by the variant caller. This lets polishing pipelines have a stopping condition to set, to stop iterative polishing when no more variants survive Merfin's filtering. Merfin depends on the accuracy of the bases in the suggested alternate sequence called by the variant caller. Long alternate insertion-like sequence from noisy long reads (for example CLR or ONT) bear a higher chance to have base errors, which are more likely to get rejected. This could be avoided by applying other tools to validate large insertions such as VaPoR⁴¹ before running Merfin. However, we note that the variant size ranges from CLR and ONT before and after polishing were well preserved as shown in Supplementary Table 6.

In addition to implementing variant evaluation and filtering in Merfin, we revised K^* , a metric based on the copy-number agreement between the reads and the assembly, to identify and analyze local expansions and collapses at each *k*-mer genome-wide. We also devised QV* and K^* completeness, quality metrics that account for over and underrepresented *k*-mers undetected by previous methods¹⁶. On the first complete human genome, we demonstrated that our approach allows orthogonal validation of both consensus sequence and variants with multiple sequencing data types.

Like all *k*-mer-based estimates, the K^* computed in Merfin is limited by the choice of *k*, which is dependent on the quality of the reads. The results presented here assume high-accuracy reads (such as Illumina) for evaluation and variant filtering and may therefore not work best with *k*-mers derived from noisy long reads (CLR reads and early ONT data). Presence of sequencing biases also results in biased K^* , such as the GC bias in Illumina reads or the GA dropouts in HiFi reads²⁵. We found Illumina reads were overall better in correcting systematic homopolymer and 2-mer microsatellite errors often introduced by HiFi reads²⁵. Yet, these effects are limited

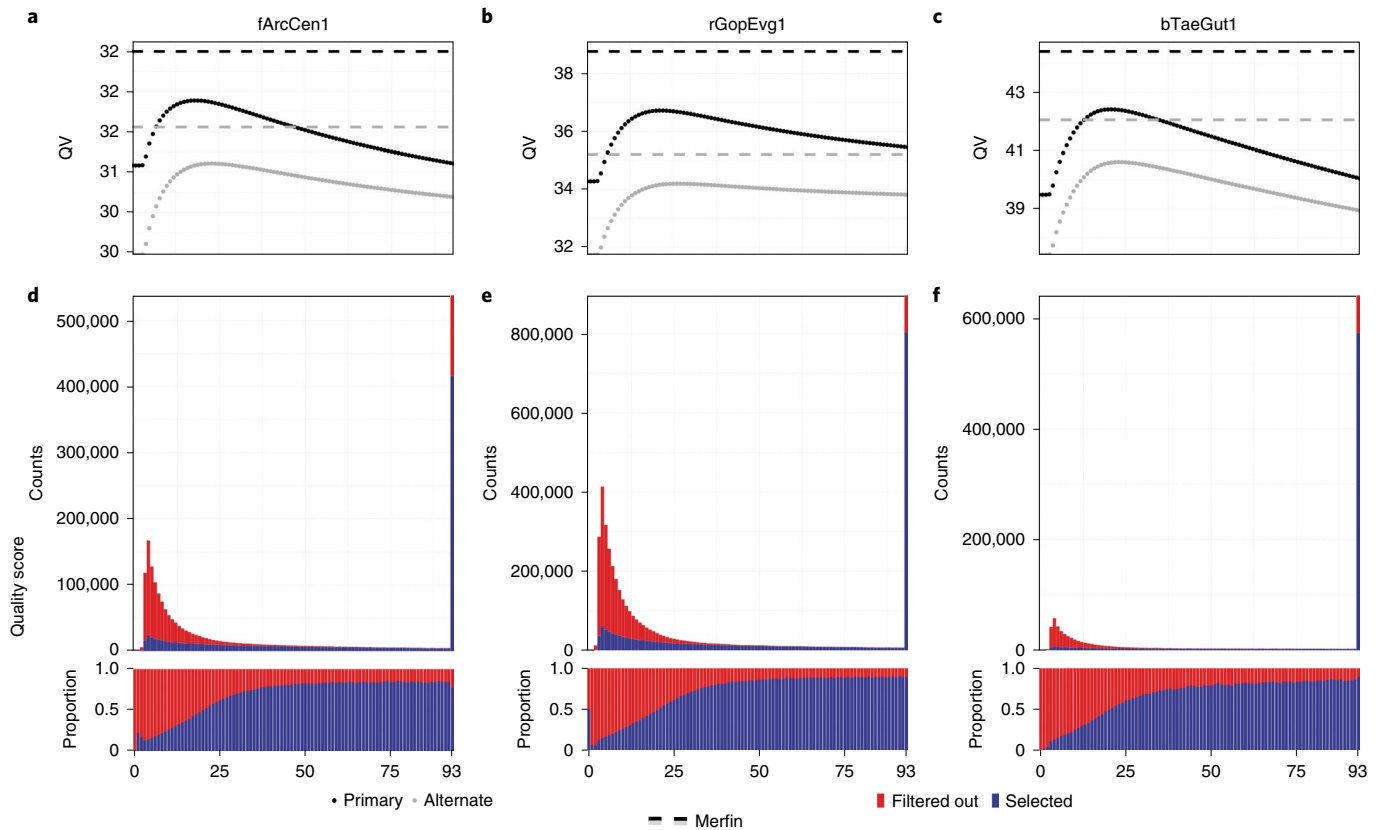


Fig. 5 | Merfin results against quality scores. **a–c**, QV after polishing as a function of hard-filtered quality score cutoff in primary (black) and alternate (gray) assembly. Results achieved with Merfin are represented by the horizontal lines for comparison. **d–f**, Number and proportion of variants by quality score selected by Merfin.

only to certain regions of the genome and it could be potentially further mitigated by methods that correct sequencing reads for known biases⁴². Accounting for these biases, integrating better methods for a more accurate estimation of the true genomic copy numbers (especially over 4×) will be a future direction for Merfin.

In parallel, the completeness of the assembly also affects the K^* . Pseudo-haploid or haploid representation of a genome may potentially lead to suboptimal evaluation because of the missing sequence. However, we argue that this is a limitation of the assemblies, rather than a limitation of the methods used to evaluate and polish them. Representing a diploid genome as a haploid or pseudo-haploid assembly introduces complications in the evaluation, as the k -mers in the consensus will not fully reflect the k -mers in the read set. Homozygous k -mers will be underrepresented and some of the alternate haplotype k -mers will be completely missing. While haploid or partially phased (such as FALCON-Unzip³⁷) assemblies can be preferred for some applications, a faithful reconstruction of the complete genome (such as using trio binning^{34,43}) should be preferred for both evaluation and comparative purposes, as well as for many biological analyses that can benefit from the presence of both haplotypes. The recent developments in assembly graphs enable the representation of complete haplotypes with enhanced accuracy and completeness⁴⁴, suggesting that assembly tools and state-of-the-art assemblies are moving in this direction. If this condition is met, the information contained in the reads can be fully harnessed to evaluate and improve genome assemblies.

Merfin provides k -mer-based variant filtering that enables higher precision in genotyping and improves assembly accuracy. This will become critical, particularly in medical genomics and

many other applications, where reliable genotyping is essential. Polishing with Merfin will also rescue assemblies built from noisy long reads when more-accurate reads are not accessible or when sequencing biases are subject to correction using complementary sequencing data.

Online content

Any methods, additional references, Nature Research reporting summaries, source data, extended data, supplementary information, acknowledgements, peer review information; details of author contributions and competing interests; and statements of data and code availability are available at <https://doi.org/10.1038/s41592-022-01445-y>.

Received: 13 July 2021; Accepted: 7 March 2022;
Published online: 31 March 2022

References

- Olson, N. D. et al. precisionFDA Truth Challenge v2: calling variants from short- and long-reads in difficult-to-map regions. Preprint at *bioRxiv* <https://doi.org/10.1101/2020.11.13.380741> (2021).
- Koboldt, D. C. Best practices for variant calling in clinical sequencing. *Genome Med.* **12**, 91 (2020).
- Guo, Y., Ye, F., Sheng, Q., Clark, T. & Samuels, D. C. Three-stage quality control strategies for DNA re-sequencing data. *Brief. Bioinform.* **15**, 879–889 (2014).
- Giani, A. M., Gallo, G. R., Gianfranceschi, L. & Formenti, G. Long walk to genomics: history and current approaches to genome sequencing and assembly. *Comput. Struct. Biotechnol. J.* **18**, 9–19 (2020).
- Rhie, A. et al. Towards complete and error-free genome assemblies of all vertebrate species. *Nature* **592**, 737–746 (2021).

6. Wenger, A. M. et al. Accurate circular consensus long-read sequencing improves variant detection and assembly of a human genome. *Nat. Biotechnol.* **37**, 1155–1162 (2019).
7. Watson, M. & Warr, A. Errors in long-read assemblies can critically affect protein prediction. *Nat. Biotechnol.* **37**, 124–126 (2019).
8. Nurk, S. et al. HiCanu: accurate assembly of segmental duplications, satellites, and allelic variants from high-fidelity long reads. *Genome Res.* **30**, 1291–1305 (2020).
9. Walker, B. J. et al. Pilon: an integrated tool for comprehensive microbial variant detection and genome assembly improvement. *PLoS ONE* **9**, e112963 (2014).
10. Chin, C.-S. et al. Nonhybrid, finished microbial genome assemblies from long-read SMRT sequencing data. *Nat. Methods* **10**, 563–569 (2013).
11. Vaser, R., Sović, I., Nagarajan, N. & Šikić, M. Fast and accurate de novo genome assembly from long uncorrected reads. *Genome Res.* **27**, 737–746 (2017).
12. McKenna, A. et al. The Genome Analysis Toolkit: a MapReduce framework for analyzing next-generation DNA sequencing data. *Genome Res.* **20**, 1297–1303 (2010).
13. Garrison, E. & Marth, G. Haplotype-based variant detection from short-read sequencing. Preprint at *arXiv* <https://arxiv.org/abs/1207.3907> (2012).
14. Poplin, R. et al. A universal SNP and small-indel variant caller using deep neural networks. *Nat. Biotechnol.* **36**, 983–987 (2018).
15. Li, H. A statistical framework for SNP calling, mutation discovery, association mapping and population genetical parameter estimation from sequencing data. *Bioinformatics* **27**, 2987–2993 (2011).
16. Rhie, A., Walenz, B. P., Koren, S. & Phillippy, A. M. Merqury: reference-free quality, completeness, and phasing assessment for genome assemblies. *Genome Biol.* **21**, 245 (2020).
17. Mapleson, D., Garcia Accinelli, G., Kettleborough, G., Wright, J. & Clavijo, B. J. KAT: a K-mer analysis toolkit to quality control NGS datasets and genome assemblies. *Bioinformatics* **33**, 574–576 (2017).
18. Kundu, R., Casey, J. & Sung, W.-K. HyPo: super fast and accurate polisher for long read genome assemblies. Preprint at *bioRxiv*. <https://doi.org/10.1101/2019.12.19.882506> (2019).
19. Jain, C. et al. Weighted minimizer sampling improves long read mapping. *Bioinformatics* **36**, i111–i118 (2020).
20. Jain, C., Rhie, A., Hansen, N., Koren, S. & Phillippy, A. M. Long read mapping to repetitive reference sequences using Winnowmap2. *Nat. Methods* (2022).
21. Phillippy, A. M., Schatz, M. C. & Pop, M. Genome assembly forensics: finding the elusive mis-assembly. *Genome Biol.* **9**, R55 (2008).
22. Nurk, S. et al. The complete sequence of a human genome. *Science* **376**, eabj6987 <https://doi.org/10.1126/science.abj6987> (2022).
23. Vollger, M. R. et al. Segmental duplications and their variation in a complete human genome. *Science* **376**, eabj6965 <https://doi.org/10.1126/science.abj6965> (2022).
24. Gershman, A. et al. Epigenetic patterns in a complete human genome. *Science* **376**, eabj5089 <https://doi.org/10.1126/science.abj5089> (2022).
25. Mc Cartney, A. M. et al. Chasing perfection: validation and polishing strategies for telomere-to-telomere genome assemblies. *Nat. Methods* (2022).
26. Jarvis, E.D. et al. Automated assembly of high-quality diploid human reference genomes. Preprint at *bioRxiv* <https://doi.org/10.1101/2022.03.06.483034> (2022).
27. Krusche, P. et al. Best practices for benchmarking germline small-variant calls in human genomes. *Nat. Biotechnol.* **37**, 555–560 (2019).
28. Ranallo-Benavidez, T. R., Jaron, K. S. & Schatz, M. C. GenomeScope 2.0 and Smudgeplot for reference-free profiling of polyploid genomes. *Nat. Commun.* **11**, 1432 (2020).
29. Cheng, H., Concepcion, G. T., Feng, X., Zhang, H. & Li, H. Haplotype-resolved de novo assembly using phased assembly graphs with hifiasm. *Nat. Methods* **18**, 170–175 (2021).
30. Huddleston, J. et al. Discovery and genotyping of structural variation from long-read haploid genome sequence data. *Genome Res.* **27**, 677–685 (2017).
31. Miga, K. H. et al. Telomere-to-telomere assembly of a complete human X chromosome. *Nature* **585**, 79–84 (2020).
32. Zook, J. M. et al. Extensive sequencing of seven human genomes to characterize benchmark reference materials. *Sci. Data* **3**, 160025 (2016).
33. Kolmogorov, M., Yuan, J., Lin, Y. & Pevzner, P. A. Assembly of long, error-prone reads using repeat graphs. *Nat. Biotechnol.* **37**, 540–546 (2019).
34. Koren, S. et al. De novo assembly of haplotype-resolved genomes with trio binning. *Nat. Biotechnol.* <https://doi.org/10.1038/nbt.4277> (2018).
35. Li, H. et al. A synthetic-diploid benchmark for accurate variant-calling evaluation. *Nat. Methods* **15**, 595–597 (2018).
36. Wagner, J. et al. Curated variation benchmarks for challenging medically relevant autosomal genes. *Nat. Biotechnol.* <https://doi.org/10.1038/s41587-021-01158-1> (2022).
37. Chin, C.-S. et al. Phased diploid genome assembly with single-molecule real-time sequencing. *Nat. Methods* **13**, 1050–1054 (2016).
38. O’Leary, N. A. et al. Reference sequence (RefSeq) database at NCBI: current status, taxonomic expansion, and functional annotation. *Nucleic Acids Res.* **44**, D733–D745 (2016).
39. NCBI. Gnomon - the NCBI eukaryotic gene prediction tool. https://www.ncbi.nlm.nih.gov/genome/annotation_euk/gnomon/ (2017).
40. Fofanov, Y. et al. How independent are the appearances of n-mers in different genomes? *Bioinformatics* **20**, 2421–2428 (2004).
41. Zhao, X., Weber, A. M. & Mills, R. E. A recurrence-based approach for validating structural variation using long-read sequencing technology. *Gigascience* **6**, 1–9 (2017).
42. Benjamini, Y. & Speed, T. P. Summarizing and correcting the GC content bias in high-throughput sequencing. *Nucleic Acids Res.* **40**, e72 (2012).
43. Yang, C. et al. Evolutionary and biomedical insights from a marmoset diploid genome assembly. *Nature* <https://doi.org/10.1038/s41586-021-03535-x> (2021).
44. Cheng, H. et al. Haplotype-resolved de novo assembly using phased assembly graphs with hifiasm. *Nat. Methods* **18**, 170–175 (2021).
45. Altomero, N. et al. Complete genomic and epigenetic maps of human centromeres. *Science* **376**, eabl4178 <https://doi.org/10.1126/science.abl4178> (2022).

Publisher’s note Springer Nature remains neutral with regard to jurisdictional claims in published maps and institutional affiliations.

This is a U.S. government work and not under copyright protection in the U.S.; foreign copyright protection may apply 2022

Methods

Genotyping benchmark. Variant calls from HG002 submitted to the precisionFDA Truth Challenge¹ were downloaded from <https://data.nist.gov/od/id/mds2-2336> (SEX9X, NFT0L, 23O09 and QUE7Q). In brief, ~35× Illumina PCR-free, ~36× PacBio HiFi and ~47× ONT reads were aligned to the human genome reference (GRCh38) with no alternates. Variants were called with GATK HaplotypeCaller v4. The unfiltered and hard-filtered dataset was downloaded and a subset of the call on chromosome 20 was extracted with bcftools v1.10.2 (<https://github.com/samtools/bcftools>). The variant calls were then benchmarked against the GIAB truth set v4.2.1 within the confident region using hap.py (v0.3.12-2-g9d128a9; <https://github.com/Illumina/hap.py>)²⁷. The GIAB variant-calling truth set and confident region for HG002 can be found in ftp://ftp-trace.ncbi.nlm.nih.gov/giab/ftp/release/AshkenazimTrio/HG002_NA24385_son/NISTv4.2.1. We used the following commands for the evaluation:

```
hap.py \
  HG002_GRCh38_1_22_v4.2.1_benchmark.chr20.vcf \
  $QRY.vcf. \
  -f HG002_GRCh38_1_22_v4.2.1_benchmark_noinconsistent.
bed \
  -r GCA_000001405.15_GRCh38_no_alt_analysis_set.fna \
  -o OUTPUT \
  -threads 24
```

Precision and recall were collected before and after filtering the variants with Merfin from the hap.py output.

To run Merfin filtering, PCR-free Illumina paired-end reads (2×250 bp) were obtained from NIST (https://ftp-trace.ncbi.nlm.nih.gov/giab/ftp/data/AshkenazimTrio/HG002_NA24385_son/NIST_Illumina_2x250bps/) and 21-mers were collected using Meryl v1.3. *K*-mers with frequency >1 were used as read *k*-mers to avoid *k*-mer collisions from sequencing errors and improved computational performance. Likewise, 21-mers from the GRCh38 primary assembly (GCA_000001405.15) were collected with Meryl and used as the sequence *k*-mers. The following commands were used to build Meryl *k*-mer databases:

```
Meryl count k=21 reads.fastq.gz output HG002.k21.
meryl
Meryl count k=21 hg38.fna output hg38.k21.meryl
```

Command lines to run Merfin can be found in the Runtime and memory section below.

Revised *K.** *K*-mers are substrings of length *k* of a given DNA sequence. Given the assembly consensus sequence, we compute all its constituent *k*-mers. Similarly, we compute all *k*-mers represented in a set of whole-genome sequencing reads from the same individual. We then ask how the frequency of each *k*-mer in the read set is mirrored in the assembly *k*-mer set. If the read set is a faithful representation of the genome (in the absence of random DNA sampling and sequencing biases), then the closer the consensus sequence is to the read set, the closer it is also to the genome that the reads were generated from. This principle can be usefully represented by our revised *K**, where for each *k*-mer in the consensus we can calculate (Fig. 1a):

K_c = *k*-mer count in the consensus sequence

K_r = *k*-mer count in the read set

To account for the uncertainty associated with the underlying Poisson sampling process, in any sequencing experiment the read set covers on average the original genome multiple times. It is therefore useful to determine the expected copy number of a particular *k*-mer in the assembly given the read set, K_a , as:

c = haploid peak from K_r histogram

K_a = the *k*-mer count expected in the consensus based on the read set, $[K_r/c]$

Note that $K_r - K_c$ expresses the number of copies of any particular *k*-mer that is underrepresented (collapsed; positive value) or overrepresented (expanded; negative value) in the assembly.

With these definitions, we can now define *K** as:

$K^* = K_r/K_c - 1$ if $K_r > K_c$ (collapsed *k*-mers)

$K^* = -(K_c/K_r - 1)$ if $K_r < K_c$ (expanded *k*-mers)

Which can be reduced to:

$K^* = (K_r - K_c) / \min(K_r, K_c)$

Note that *K** converges to 0 if the *k*-mer frequency in the assembly matches the expected copy number in the reads. Missing *k*-mers (found in the assembly but not in the read set) have a special behavior, with *K** being 'undefined' for $K_r = 0$.

Probabilistic *K*-mer copy-number estimation. To estimate *k*-mer copy number in the genome, we modified Genomescope2 (ref. ²⁸) to obtain the associated probability at each K_r . Our additions were subsequently integrated in the current version of Genomescope2 (<https://github.com/tbenavil/genomescope2.0>). Unmodified fitted model one- to four-copy *k*-mer distributions were used to infer the probability that a particular *k*-mer frequency observed in the read set implied a particular copy *k*-mer in the genome.

QV estimation using the *K.** An average genome-wide QV* is obtained by counting all *k*-mers not present compared to the expected copy number estimated

from the read set. We collect all *k*-mers excessively found in the assembly (K_e) and estimate the error rate given all *k*-mers in the assembly (K_{total}).

$K_e = \sum K_c - K_r$ when $K_c > K_r$ for all positions in the assembly

The Phred-scaled QV* can be computed using the implementation in Merquy¹⁶.

We follow the implementation in Merquy and compute the probability *P* that a base in the assembly is correct and in its expected frequency:

$P = ((K_{total} - K_e) / K_{total})^{1/k}$

Which leads to error rate *E* being:

$E = 1 - P$

Hence the Phred-scaled QV* becomes:

$QV^* = -10 \log E$

Assembly completeness using the *K.** To estimate completeness, we collect all *k*-mers that should be present but are absent from the assembly. Unlike Merquy, we account for the *k*-mer frequency and count any *k*-mer that should be added to meet the expected frequency from the reads K_a .

$K_a = \sum (K_r - K_c)$ when $K_r > K_c$ for all K_r , including $K_c = 0$

We compute the completeness (Comp) given all K_r :

$Comp (\%) = (K_r - K_a) / K_r = 1 - K_a / K_r$

Sequence data. For the HG002 results, data can be found at https://github.com/human-pangenomics/HG002_Data_Freeze_v1.0. For the VGP datasets, PacBio CLR and 10X Genomics linked reads can be found at <https://vgp.github.io/genomeark/>.

Evaluation of CHM13 assemblies. All scripts used for CHM13 evaluation can be found here: <https://github.com/gi777/misc/tree/master/merfin>.

Briefly, we generated genome-wide *K** tracks using Merfin option `-dump` (`merfin_dump.sh`). *K*-mer counts databases for both the assemblies and the raw Illumina and HiFi reads were computed using Meryl (<https://github.com/marbl/meryl>). Peak values of 106.8 and 31.8 derived as the *kcov* value from Genomescope were used for Illumina and HiFi *k*-mers, respectively, which is now obtainable with Genomescope2 `-p 1` (commit version `fdeb89178d506c9af2c5d0d103e0135a164889a3`). The tracks were converted to bigWig and loaded in IGV³⁶ for visualization. We used a custom script (`simplify_dump.sh`) to count the number of bases with the same *K** values for both Illumina and HiFi *k*-mers, which were then used to generate the genome-wide *K** comparison. The titration experiment was performed downsampling the reads with the `'seqtk sample'` command (<https://github.com/lh3/seqtk>, v1.3).

Variant calling and polishing of HG002 assemblies. Variant calling and polishing of HG002 assemblies was performed using medaka v1.2.6 (<https://github.com/nanoporetech/medaka>) using the models specified in Supplementary Table 3 for each dataset. Medaka was first run in the consensus mode (`medaka_consensus`) and subsequently in the variant mode (`medaka_variant`) to generate the VCF of the variant calls. Illumina 21-mers from the HG002 benchmark were re-used for evaluation and filtering with Merfin. A Medaka-filtered variant set was then used in conjunction with bcftools v1.9 in the consensus mode with the `-H 1` option to generate a consensus sequence. The same procedure was followed for the Merfin assemblies, except that Merfin was used to filter Medaka VCF before consensus generation. Polishing was repeated twice and in the second round the assembly polished with Merfin was used as reference. Additional best practices for running Merfin are in the GitHub repository (<https://github.com/aranghie/merfin/wiki/Best-practices-for-Merfin>).

Assembly-based small-variant-calling assessment. We used dipcall v0.3 (<https://github.com/lh3/dipcall>) to generate the small variants from the assembly. Dipcall takes a diploid assembly and a reference genome to produce a VCF that contains all variants that are present in the assembly compared to the reference. We then compared the variant calls against the GIAB truth set v4.2.1 using hap.py as described in the Genotyping benchmark session. We used the following commands for the evaluation:

```
./run-dipcall <output_prefix> <GRCh38.fa> <pat.fa>
<mat.fa> -t 8 -x hs38.PAR.bed
hap.py HG002_GRCh38_1_22_v4.2.1_benchmark.vcf.gz \
  DIPCALL_OUTPUT.dip.vcf.gz \
  -f HG002_GRCh38_1_22_v4.2.1_benchmark_noinconsistent.
chr20.bed \
  -r GCA_000001405.15_GRCh38_no_alt_analysis_set.fna -o
OUTPUT \
  -pass-only-engine=vcfEval-threads=32
```

Variant calling and polishing of VGP assemblies. While the original assemblies were generated with different versions of the VGP pipeline⁵ (<https://github.com/VGP/vgp-assembly/tree/master/pipeline>), to polish the assemblies of the flier cichlid (v1.0), the Goode's thornscrub tortoise (v1.5) and the zebra finch (v1.6) with Merfin we used the VGP pipeline v1.6 (Extended Data Fig. 7). In

the first round of polishing, PacBio CLR reads were aligned with pbmm2 v1.0.0, variants were called with variantCaller v2.3.3 (Arrow) with the `-o ${asm}.vcf` option. A custom script (https://github.com/arangrhie/merfin/blob/master/scripts/reformat_arrow/) included in Merfin was used to properly format the VCF (reshape_arrow.sh). The 21-mer databases for both the assemblies and the 10X linked reads were generated with Meryl. The 10X barcodes were trimmed from the reads using the script available in Meryl. The haploid 21-mer coverage and the lookup tables were computed using our modified Genomescope2 script included in Merfin:

```
Rscript $merfin/lookup.R ${asm}.21.meryl.hist 21
${asm}.21.lookup 2
```

Similarly to HG002, the consensus was generated with bcftools v1.9 using the filtered VCF generated by Merfin. The same strategy was applied for the other polishing steps, except that Longranger v2.2.2 was used for mapping the 10X Genomics linked reads and Freebayes v1.3.1 (<https://github.com/freebayes/freebayes/>) for variant calling.

For variant calling and polishing of the zebra finch trio, curated primary (bTaeGut2.pri.cur.20191112.fasta) and alternate (bTaeGut2.alt.cur.20181019.fasta) pseudo-haploid assemblies were downloaded from GenomeArk (https://genomeark.s3.amazonaws.com/index.html?prefix=species/Taeniopygia_guttata/bTaeGut2/assembly_curated/). The 10X linked reads were aligned with Freebayes on the primary and alternate assembly using Longranger with default options. Freebayes calls were filtered using Bcftools v1.9 with the `-i ' (GT="AA" || GT="Aa") '` option before Merfin filtering. *K*-mer counts databases for both the assemblies and the raw Illumina reads were computed using Meryl and Merfin was run with a peak value of 35.2 derived as the *kcov* value from Genomescope2.

Evaluation of the assemblies. QV and phasing analyses of HG002 and zebra finch trios were performed using Merquy¹⁶ (<https://github.com/marbl/merquy/>) in the trio mode using 21-mers and default parameters. Similarly, primary and alternate scaffolds of the VGP assemblies were separated and Merquy QV was estimated on both using 21-mers and default parameters.

Gene annotation of VGP assemblies. Annotation was performed using the National Center for Biotechnology Information annotation pipeline⁵, using the same transcript, protein and RNA-seq input evidence for the annotation of the unpolished, polished and Merfin assemblies of each species. For *T. guttata*, a total of 100,000 *T. guttata* expressed sequence tags, GenBank and known RefSeq³⁸ and 10 billion same-species reads for over 13 tissues were aligned to the genome, in addition to all GenBank Aves proteins, known Aves, human and *Xenopus* RefSeq proteins and RefSeq model proteins for *Parus major*, *Gallus gallus*, *Columbia livia* and *Pseudopodoces humilis*. For *G. evgoodei*, 1.22 billions RNA-seq reads from five tissue types from *Gopherus* and *Chelonoidis* species were aligned to the assemblies in addition to all known RefSeq proteins from human, *Xenopus* and *Sauropsida* and model RefSeq proteins from *Chrysemys picta*, *Pelodiscus sinensis*. For *A. centrarchus*, 476 million same-species RNA-seq reads from nine tissue types were aligned to the assemblies in addition to all *Actinoipterygii* GenBank proteins, human and *Actinoipterygii* known RefSeq proteins and *Oryzias latipes*, *Oreochromis niloticus*, *Monopterus albus*, *Xiphophorus maculatus* model RefSeq proteins. In brief, the genome sequences were masked with Windowmasker⁴⁷ before annotation. Transcription RNA-seq data were aligned with BLAST⁴⁸ followed by Splign⁴⁹ and RefSeq and GenBank proteins were aligned using Blast and ProSplign. The gene model's structure and boundaries were obtained with Gnomon (https://www.ncbi.nlm.nih.gov/genome/annotation_euk/gnomon/) by manipulating a hidden Markov model trained on the species. Transfer RNAs were predicted with tRNAscan-SE v1.23 (ref.⁵⁰) and small noncoding RNAs were predicted with RFAM v12.0 hidden Markov models using cmsearch from the Infernal package⁵¹.

Runtime and memory requirements. Computational requirements for *k*=21 and *k*=31 are reported in Supplementary Tables 10–12. Commands used were:
HG002 GIAB benchmark:

```
Merfin -filter -sequence GRCh38_no_alt_analysis_set_clean.fasta -seqmers hg38.meryl -readmers HG002.k21.[gt1.]meryl -vcf $in_vcf -debug -output $out
```

T2T-CHM13v1.0 assembly evaluation:

```
merfin -hist -threads 24 -sequence $fasta -seqmers $fasta.k21.[gt1.]meryl -readmers chm13.k21.[gt1.]meryl -prob lookup_table.k21.txt -peak 106.7 -output $out.hist
merfin -hist -sequence $fasta -seqmers $fasta.k31.[gt1.]meryl -readmers chm13.k31.[gt1.]meryl -prob lookup_table.k31.txt -peak 99.59 -output $out.hist
```

fArcCen1 Arrow polishing:

```
merfin -polish -sequence fArcCen1_s4.fasta.gz -readmers fArcCen1.k21.[gt1.]meryl -prob lookup_table.k21.txt -peak 10.8 -vcf fArcCen1_s4.resshaped.vcf.gz -output $out
merfin -polish -sequence fArcCen1_s4.fasta.gz -seqmers $seqmers -readmers fArcCen1.k31.[gt1.]meryl -prob lookup_table.k31.txt -peak 9.1 -vcf fArcCen1_s4.resshaped.vcf.gz -output $out
```

Output variants from the fArcCen1 experiment were compressed with bcftools (`bcftools consensus -f $fa -H 1 $vcf.gz > $out.fasta`) and used for generating the polished consensus. Evaluation of the polished fArcCen1 experiments were performed on *k*=21 with Merfin options `-hist -prob lookup_table.k21.txt -peak 10.8 -readmers fArcCen1.k21.meryl`. All probability lookup tables were generated with Genomescope2 with options `-fitted_hist -p 1` (ploidy=1) for CHM13 evaluation. Experiments were run on Biowulf, NIH HPC clusters with 24 threads allowed. Maximum memory and detailed cluster specifications are in Supplementary Tables 10–12.

Reporting Summary. Further information on research design is available in the Nature Research Reporting Summary linked to this article.

Data availability

HG002 variant-call data were downloaded from <https://data.nist.gov/od/id/mds2-2336> (SEX9X, NFT0L, 23O09 and QUE7Q). Sequencing data and assemblies for CHM13, HG002 and VGP genomes are available at <https://github.com/marbl/CHM13>, https://github.com/human-pangenomics/HG002_Data_Freeze_v1.0 and <https://vgp.github.io/>.

Source data used for generating all figures in this manuscript are available at <https://github.com/gf777/misc/tree/master/merfin/paper/figures>. The *K** tracks for HiFi and Illumina of the CHM13 are browsable in the associated UCSC browser (http://genome.ucsc.edu/cgi-bin/hgTracks?db=hub_2395475_t2t-chm13-v1.1). All variant calls used in the genotyping benchmarks, *k*-mer databases, fitted histogram tables and *K** tracks are available to download at https://s3-us-west-2.amazonaws.com/human-pangenomics/index.html?prefix=publications/MERFIN_2021/ with a step-by-step guideline available at <https://github.com/arangrhie/merfin/wiki/Best-practices-for-Merfin>. All data are publicly open for download with no restrictions.

Code availability

A stable release and the source code for Merfin and examples from this work are available under Apache License 2.0 at GitHub (<https://github.com/arangrhie/merfin>) and Zenodo (<https://doi.org/10.5281/zenodo.5527270>)⁵². The only dependency is the *k*-mer counter Meryl, which comes with the release. Merfin can be run in five modes (1) the `-filter` mode scores each variant or variants within distance *k* and their combinations by error *k*-mers for improved genotyping; (2) the `-completeness` mode generates completeness metrics; (3) the `-dump` mode computes *K_c*, *K_r*, *K** for each base in the assembly along with QV and QV* for each sequence; (4) the `-hist` mode provides a *K** histogram and genome-wide QV and QV* averages; and (5) the `-polish` mode scores each variant or variants within distance *k* and their combinations by the *K** for polishing. Merfin is fully parallelized using OpenMP. A combination of bash and Rscript used for data analysis and visualization is available at <https://github.com/gf777/misc/tree/master/merfin/paper/figures>. A Code Ocean capsule of the package is provided (<https://doi.org/10.24433/CO.2292349.v1>)⁵³.

References

- Robinson, J. T. et al. Integrative genomics viewer. *Nat. Biotechnol.* **29**, 24–26 (2011).
- Morgulis, A., Gertz, E. M., Schäffer, A. A. & Agarwala, R. WindowMasker: window-based masker for sequenced genomes. *Bioinform. Oxf. Engl.* **22**, 134–141 (2006).
- Altschul, S. F., Gish, W., Miller, W., Myers, E. W. & Lipman, D. J. Basic local alignment search tool. *J. Mol. Biol.* **215**, 403–410 (1990).
- Kapustin, Y., Souvorov, A., Tatusova, T. & Lipman, D. Splign: algorithms for computing spliced alignments with identification of paralogs. *Biol. Direct* **3**, 20 (2008).
- Lowe, T. M. & Eddy, S. R. tRNAscan-SE: a program for improved detection of transfer RNA genes in genomic sequence. *Nucleic Acids Res.* **25**, 955–964 (1997).
- Nawrocki, E. P. et al. RFAM 12.0: updates to the RNA families database. *Nucleic Acids Res.* **43**, D130–D137 (2015).
- Formenti, G., Rhie, A. & Walenz, B. *arangrhie/merfin: Merfin v1.0*. Zenodo <https://doi.org/10.5281/zenodo.5527270> (2021).

53. Formenti, G., Rhie, A. & Walenz, B. Merfin - improved Arrow polishing through vcf filtering and Genomescope2 kmer models. *Code Ocean* <https://doi.org/10.24433/CO.2292349.v1> (2022).

Acknowledgements

We thank T. Rhyker Ranallo-Benavidez and M.C. Schatz for the useful discussion on adapting Genomescope2 models. We also thank the communities of the T2T, HPRC and VGP consortia for their constant support. G.F. and E.D.J. were supported by Rockefeller University and HHMI funds. A.R., B.P.W., S.K. and A.M.P. were supported by the Intramural Research Program of the National Human Genome Research Institute, National Institutes of Health (NIH) (1ZIAHG200398). The work of F.T.-N. was supported by the Intramural Research Program of the National Library of Medicine, NIH. K.S. was supported by NIH/NHGRI (R01HG010485, U41HG010972, U01HG010961, U24HG011853 and OT2OD026682). E.W.M. was partially supported by the German Federal Ministry of Education and Research (01IS18026C). Part of this work used the computational resources of the NIH HPC Biowulf cluster (<https://hpc.nih.gov>).

Author contributions

A.R., G.F., B.P.W. and E.W.M. implemented Merfin. G.F. and A.R. performed the validation analyses. K.S. performed the GIAB variant-calling analysis on HG002. F.T.

generated the gene annotations for the VGP genomes. S.K. contributed to the conceptual development. G.F. and A.R. wrote the manuscript. G.F., A.R., E.D.J. and A.M.P. conceived the study. All authors reviewed, edited and approved the manuscript.

Competing interests

S.K. has received travel funds to speak at symposia organized by Oxford Nanopore. The remaining authors declare no competing interests.

Additional information

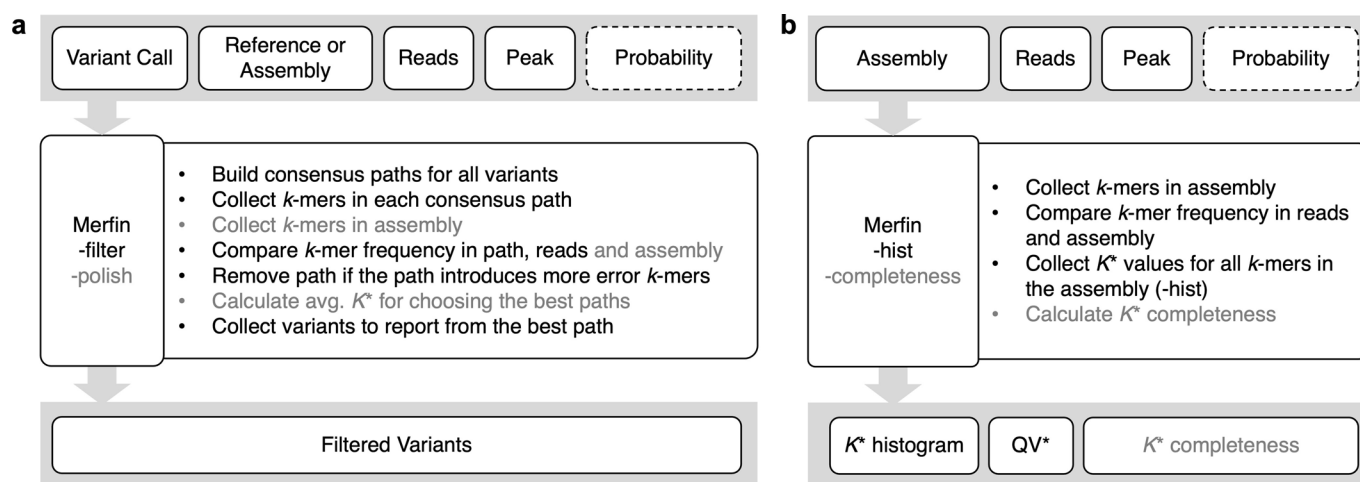
Extended data is available for this paper at <https://doi.org/10.1038/s41592-022-01445-y>.

Supplementary information The online version contains supplementary material available at <https://doi.org/10.1038/s41592-022-01445-y>.

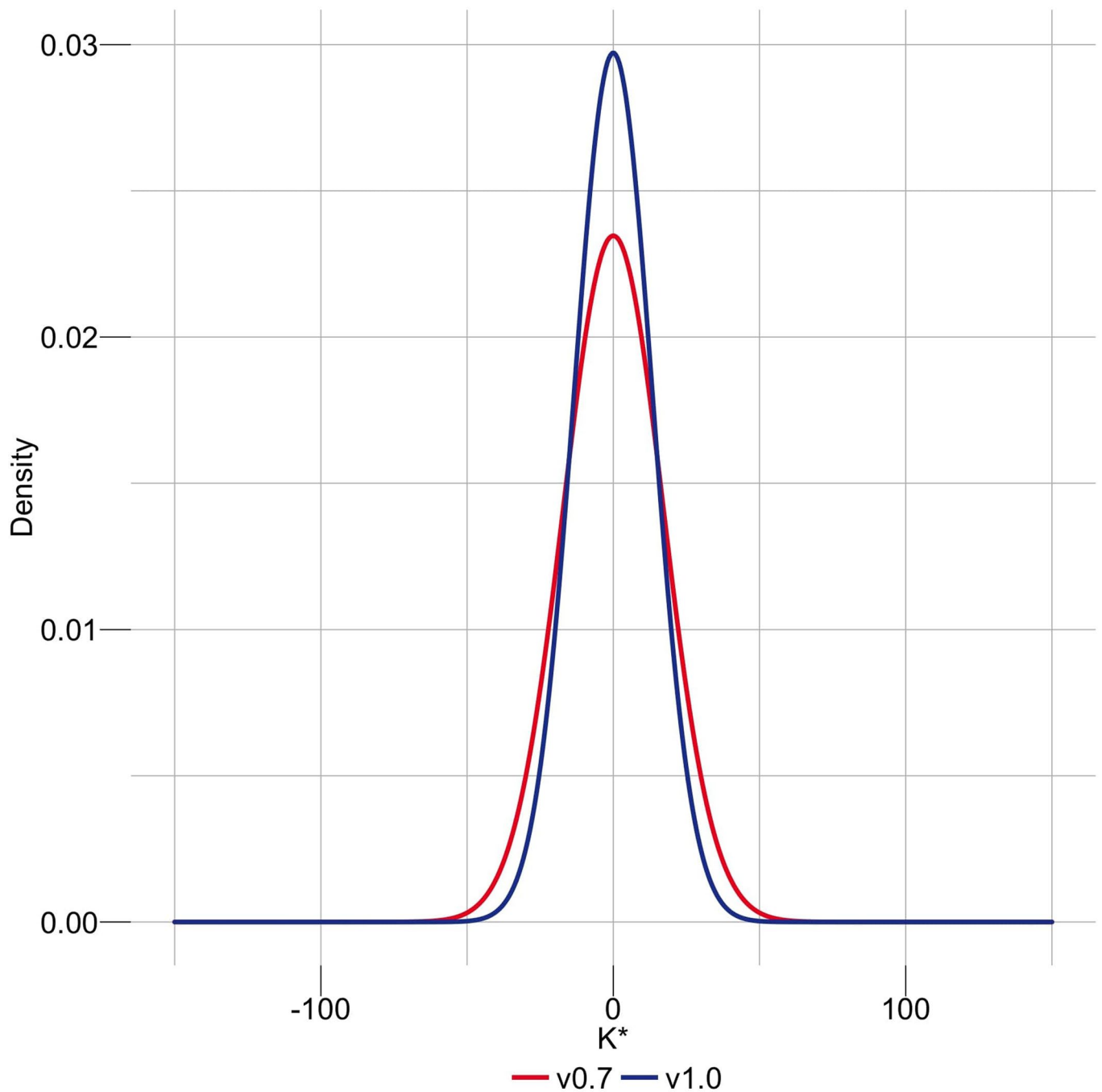
Correspondence and requests for materials should be addressed to Giulio Formenti or Arang Rhie.

Peer review information *Nature Methods* thanks Chuan-Le Xiao and the other, anonymous, reviewer for their contribution to the peer review of this work. Primary Handling editor: Lin Tang, in collaboration with the Nature Methods team. Peer reviewer reports are available.

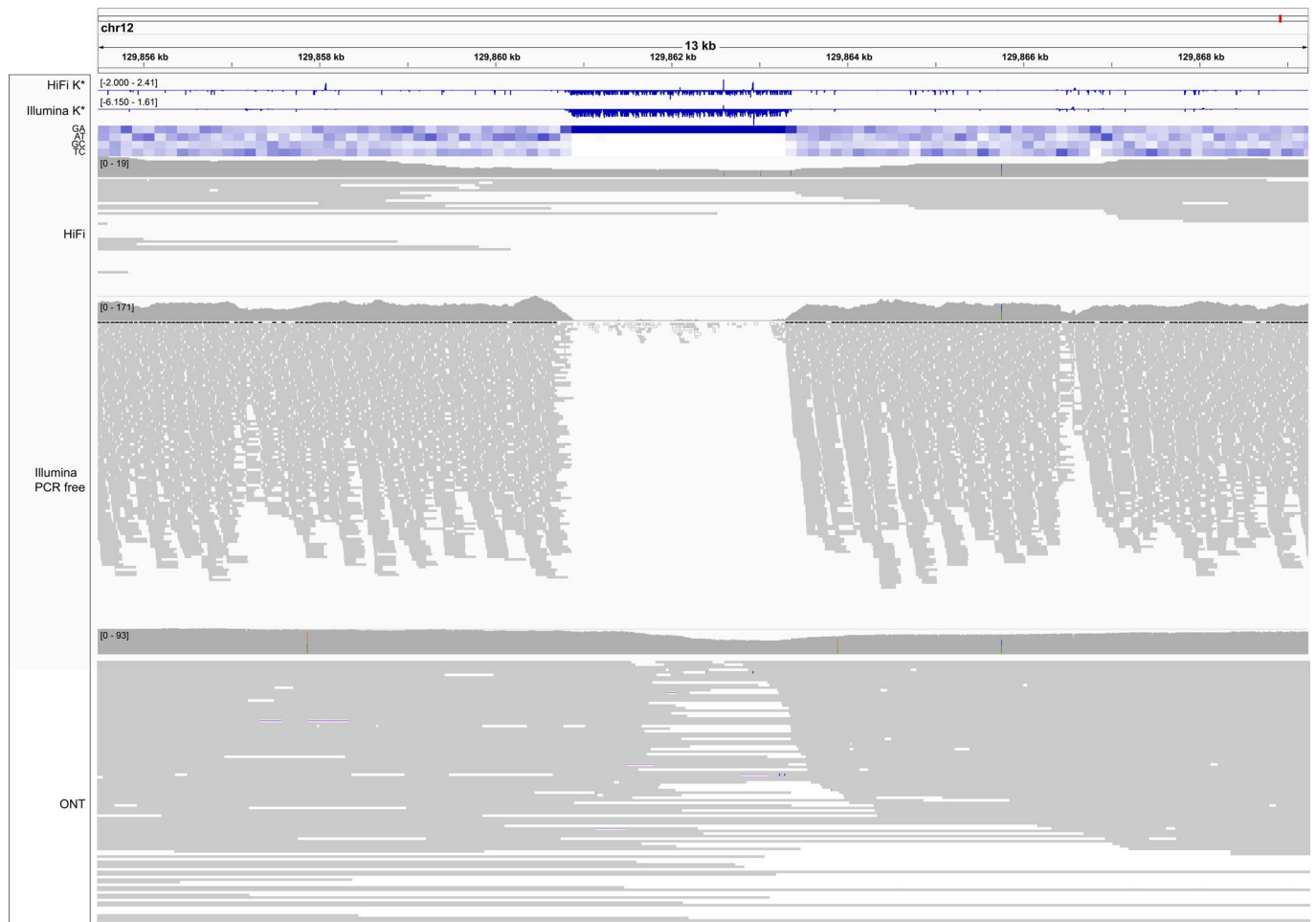
Reprints and permissions information is available at www.nature.com/reprints.



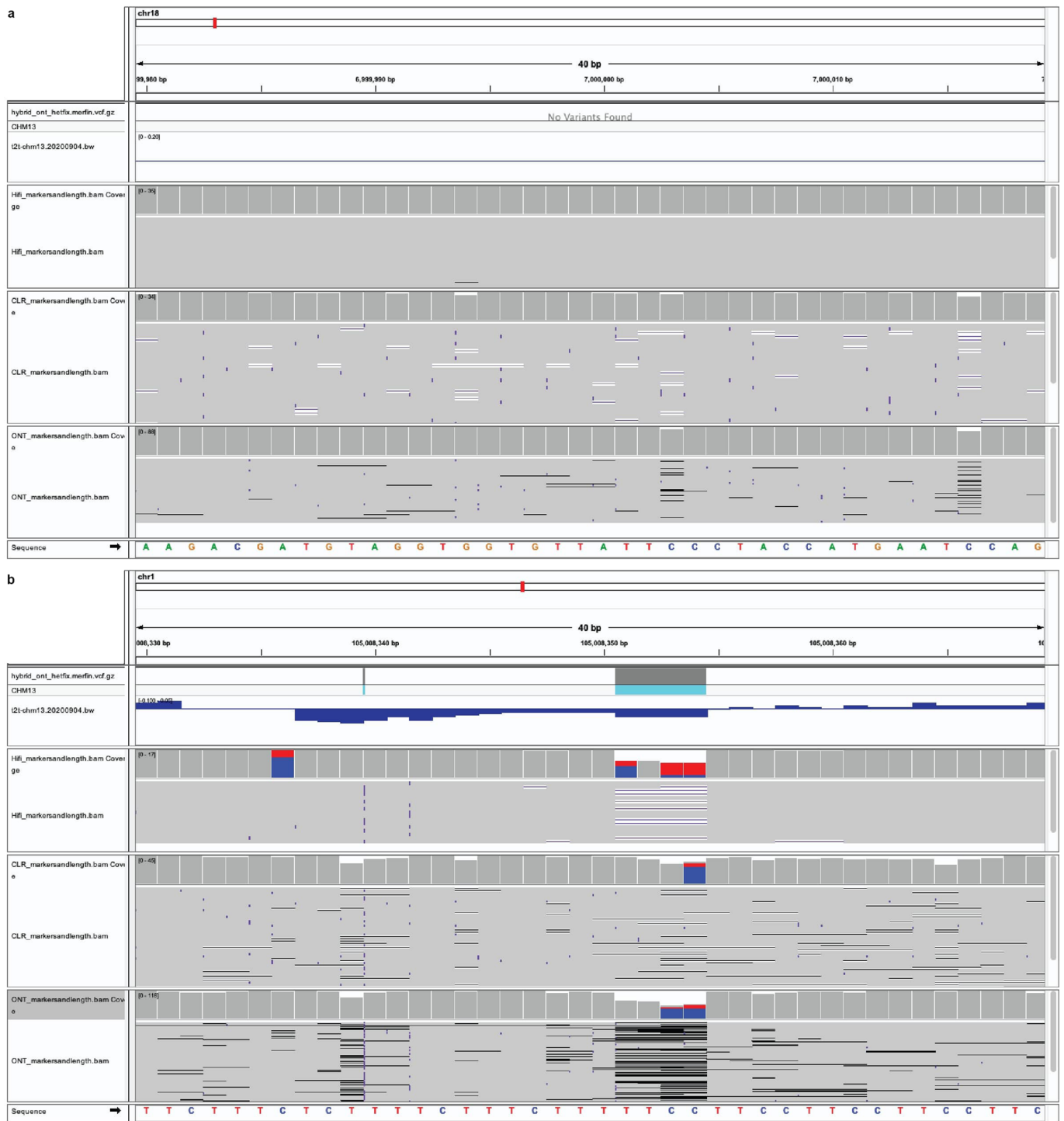
Extended Data Fig. 1 | Flowchart diagram of each mode in Merfin. Text inside gray boxes on the top represents input files required (solid) or optional (dashed) for Merfin. **a**, genotyping (-filter) and polishing (-polish) modes. **b**, K^* histogram (-hist) and K^* completeness (-completeness) modes. Steps listed in bullet points are marked in gray if it is only applicable in -polish (**a**) or -completeness (**b**) mode.



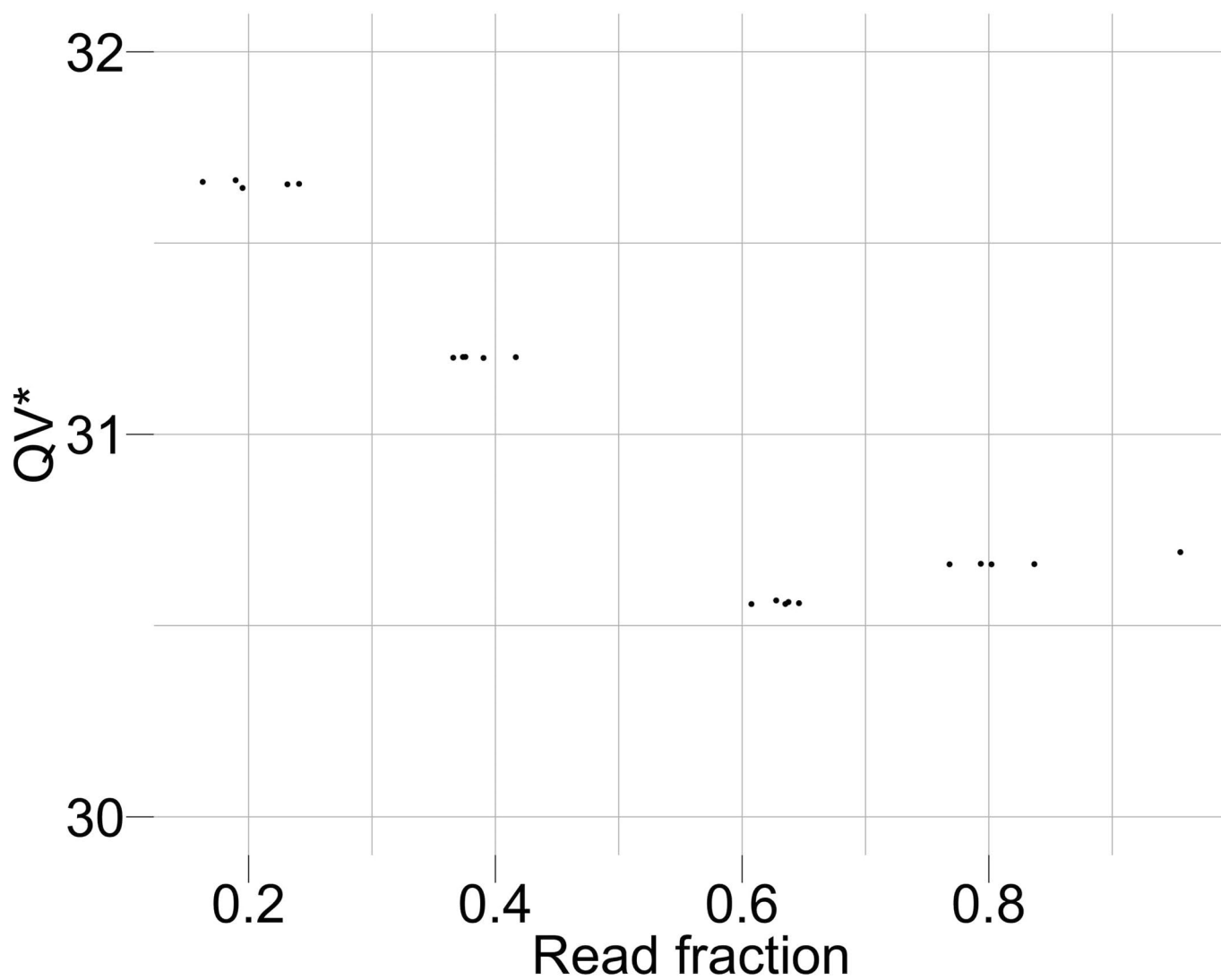
Extended Data Fig. 2 | Genome-wide density distribution of the K^* using Illumina k -mers. When the assembly is in agreement with the raw data, the K^* is normally distributed with mean 0 and the smaller the standard deviation the higher the agreement. T2T-CHM13v1.0 shows a less dispersed distribution of the K^* compared to v0.7.



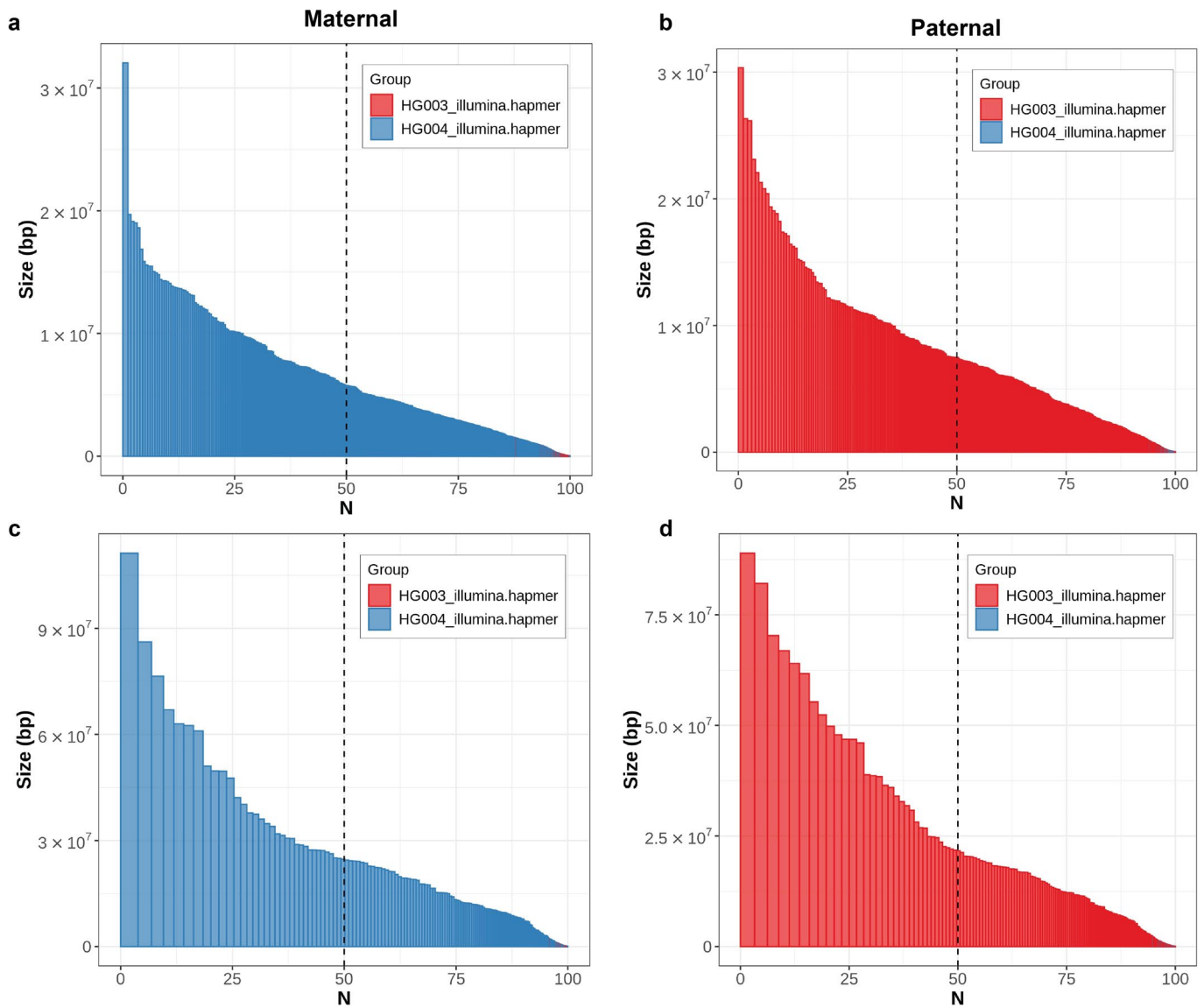
Extended Data Fig. 3 | A region of negative K^* highlighting sequencing bias. An example of low coverage in both HiFi and Illumina reads associated with high guanine content, and specifically a GA-rich repeat (heatmap). GA bias has been reported in PacBio HiFi data, and results in gaps in the assembly that in CHM13 were filled with Nanopore data²². The K^* both from HiFi and Illumina k -mers (top tracks) recapitulate the coverage drop. Nanopore coverage appears less affected. Position Chr. 12:~129,862,000 bp.



Extended Data Fig. 4 | The K^* can identify issues in the assembly at the base level. **a, 40 bp window with K^* close to 0, highlighting perfect agreement of the assembly with the raw reads. Position Chr18:-7,000,000 bp. **b**, A region of negative K^* in coincidence with two heterozygous indels. Position Chr1:-105,008,350 bp.**

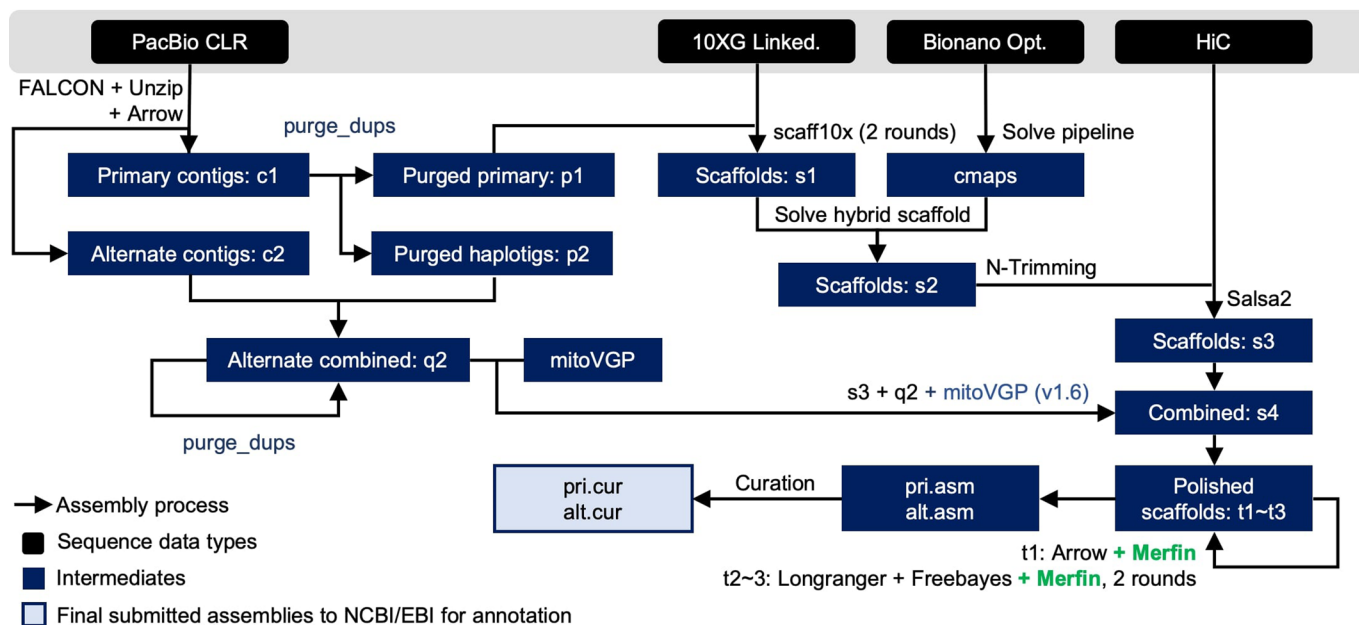


Extended Data Fig. 5 | Coverage titration experiment and impact on QV^* . The QV^* is only marginally influenced by the coverage of the dataset being considered.

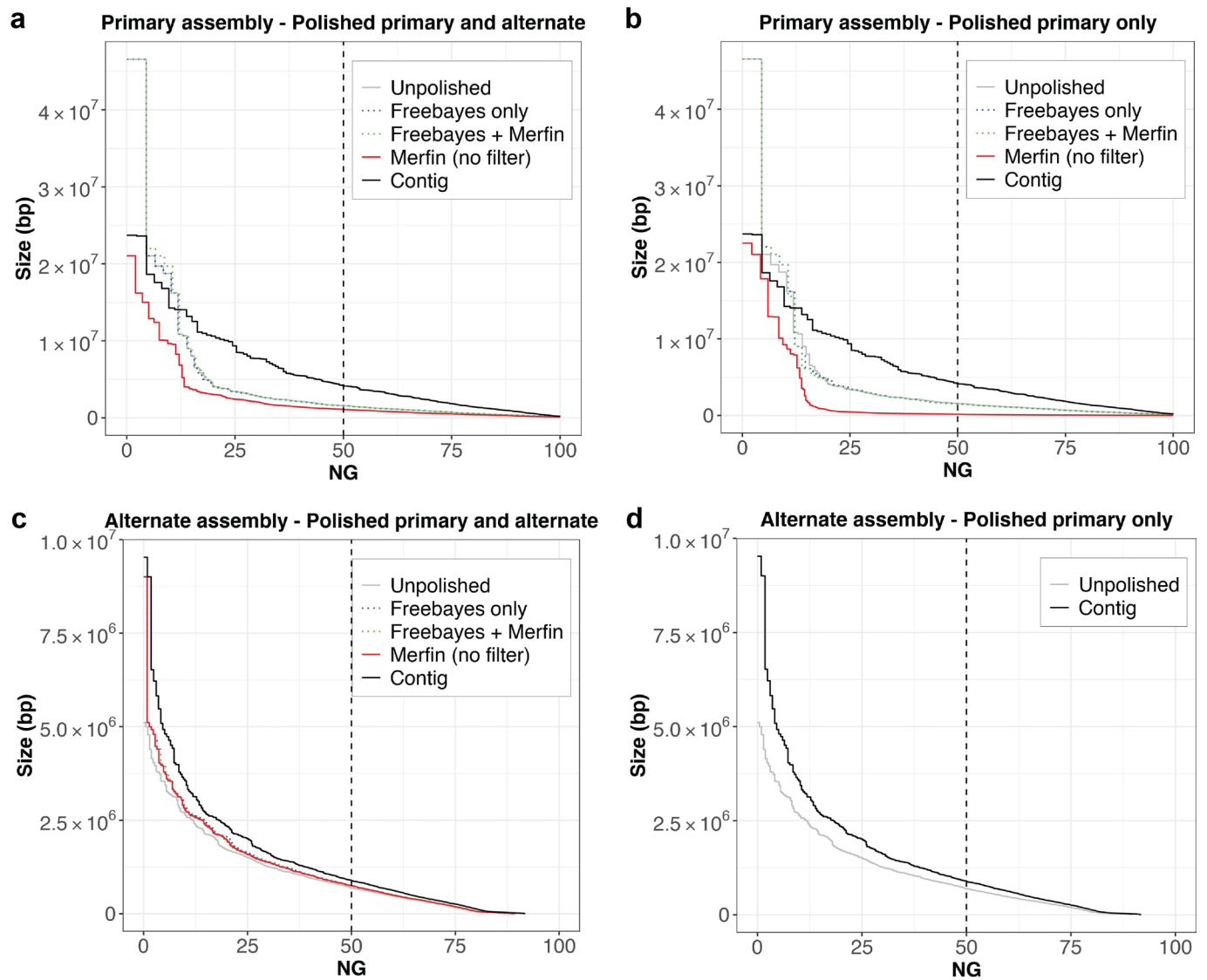


Extended Data Fig. 6 | Haplotype phasing before and after polishing with Merfin. In both parental assemblies, the haplotypes remained fully phased, and the size of the blocks substantially increased compared to the unpolished version (**a,b**) after polishing with Merfin (**c,d**). A theoretical human genome size of 3.1 Gbp was used to normalize NG^* values.

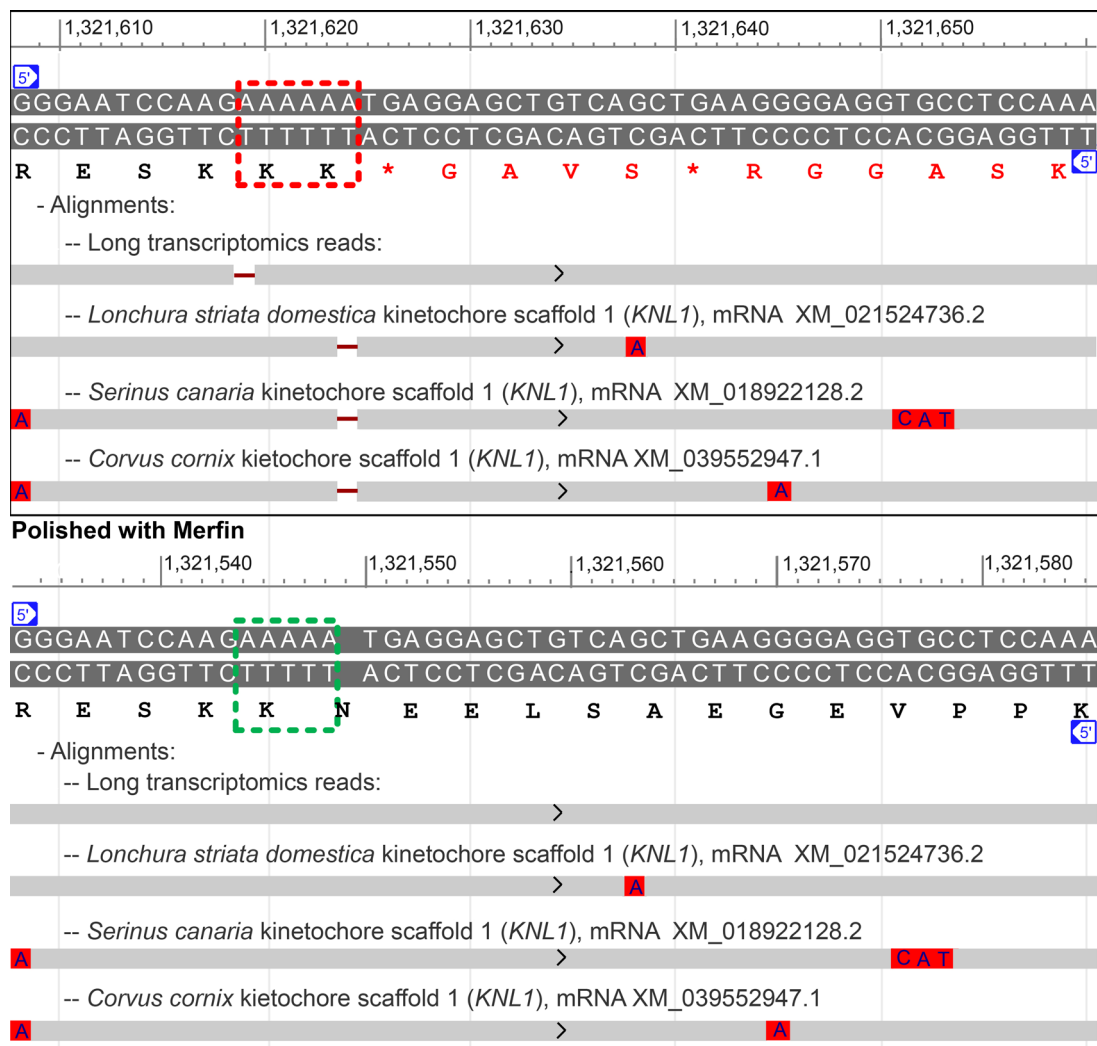
VGP assembly standard pipeline (v1.6 - v1.7)



Extended Data Fig. 7 | VGP assembly pipeline. Compared to the previous v1.6, the introduction of Merfin in v1.7 (green) resulted in a minimal change of the workflow, but in a generalized improvement in QV scores and gene annotations. Pipeline available at <https://github.com/VGP/vgp-assembly>.



Extended Data Fig. 8 | Phase block analysis of zebra finch pseudo-haploid assembly. **a**, Phase blocks in the primary assembly after mapping the reads to both the primary and alternate assemblies. **b**, Phase blocks in the primary assembly after mapping the reads to the primary only. **c**, Phase blocks in the alternate assembly after mapping the reads to both the primary and alternate assemblies. **d**, Phase blocks in the alternate assembly. In all cases, the application of Merfin filtering minor heterozygous variants (green) leads to block sizes better or comparable to prior polishing methods alone (blue). Unpolished assembly in gray. Results of Merfin without filtering in red. A genome size of ~1.03 Gbp derived from Genomescope2 was used to normalize NG* values.



Extended Data Fig. 9 | Effect of merfin correction on the kinetochore scaffold 1 (*KNL1*) annotation. **a**, Deleterious presence of an extra A around position 1,321,620 of scaffold_7 (red box) in the polished, non-merfin-corrected sequence is indicated by a 1-base gap in the alignments of zebra finch PacBio IsoSeq SRR8695295.20794.1 and *KNL1* transcripts from three other Passeriformes songbirds. This insertion causes a disruption in the frame and a premature stop codon in the translated sequence (see amino acid sequence in red). **b**, Corresponding span in the merfin-corrected assembly, with gapless alignments of the IsoSeq read and Passeriformes transcripts, and uninterrupted translation.

Reporting Summary

Nature Research wishes to improve the reproducibility of the work that we publish. This form provides structure for consistency and transparency in reporting. For further information on Nature Research policies, see our [Editorial Policies](#) and the [Editorial Policy Checklist](#).

Statistics

For all statistical analyses, confirm that the following items are present in the figure legend, table legend, main text, or Methods section.

n/a Confirmed

- The exact sample size (n) for each experimental group/condition, given as a discrete number and unit of measurement
- A statement on whether measurements were taken from distinct samples or whether the same sample was measured repeatedly
- The statistical test(s) used AND whether they are one- or two-sided
Only common tests should be described solely by name; describe more complex techniques in the Methods section.
- A description of all covariates tested
- A description of any assumptions or corrections, such as tests of normality and adjustment for multiple comparisons
- A full description of the statistical parameters including central tendency (e.g. means) or other basic estimates (e.g. regression coefficient) AND variation (e.g. standard deviation) or associated estimates of uncertainty (e.g. confidence intervals)
- For null hypothesis testing, the test statistic (e.g. F , t , r) with confidence intervals, effect sizes, degrees of freedom and P value noted
Give P values as exact values whenever suitable.
- For Bayesian analysis, information on the choice of priors and Markov chain Monte Carlo settings
- For hierarchical and complex designs, identification of the appropriate level for tests and full reporting of outcomes
- Estimates of effect sizes (e.g. Cohen's d , Pearson's r), indicating how they were calculated

Our web collection on [statistics for biologists](#) contains articles on many of the points above.

Software and code

Policy information about [availability of computer code](#)

Data collection AWS command line interface tool (AWS CLI) was used to download data from the Amazon S3 bucket.

Data analysis

Genotyping benchmark was performed with happy.py v0.3.12 (<https://github.com/illumina/hap.py>) using the GIAB truth set v4.2.1 for HG002 available from NIST (ftp://ftp-trace.ncbi.nlm.nih.gov/giab/ftp/release/AshkenazimTrio/HG002_NA24385_son/NISTv4.2.1). All variant calls throughout the analysis were manipulated with bcftools v1.10.2 (<https://github.com/samtools/bcftools>) to subset for Chr. 20 in benchmarking, filtering, and generating the polished consensus. K-mer databases were generated using Meryl v1.3 (<https://github.com/marbl/meryl>). Once k-mers were collected from the reads, GenomeScope2 with --fitted_hist, available from commit ver. fdeb89178d506c9af2c5d0d103e0135a164889a3. Read downsampling for the titration experiment was performed with seqtk v1.3 (<https://github.com/lh3/seqtk>).

Variant calling and polishing was performed using Medaka v1.2.6 (<https://github.com/nanoporetech/medaka>). Assembly-based small variant callings were performed with dipcall v0.3 (<https://github.com/lh3/dipcall>). Benchmarking against the GIAB truth set was performed as for the genotyping benchmarks. Large variant (error) callings from the VGP PacBio CLR assemblies were performed with pbmm2 v1.0.0 and variantCaller v2.3.3 (Arrow), with the output vcf transformed using a custom script (reshape_arrow.sh, https://github.com/arangrhie/merfin/blob/master/scripts/reformat_arrow/). Short error callings were performed with 10X Genomics reads using longranger v2.2.2 and FreeBayes v1.3.1. Annotation was performed using the NCBI RefSeq annotation pipeline (https://www.ncbi.nlm.nih.gov/genome/annotation_euk/gnomon/).

Custom bash and R-scripts for plotting to generate manuscript figures are available at <https://github.com/gf777/misc/tree/master/merfin/paper/figures> along with all data used for plotting.

A stable release and the C++ source code for Merfin, and examples from this work are available under Apache License 2.0 (<https://github.com/arangrhie/merfin>). The only dependency is the k-mer counter Meryl, which comes with the release. Merfin can be run in five modes: 1) the -filter mode scores each variant, or variants within distance k and their combinations by error k-mers for improved genotyping; 2) the -completeness mode generates completeness metrics; 3) the -dump mode computes KC, KR, K^* for each base in the assembly along

with QV and QV* for each sequence; 4) the -hist mode provides a K* histogram and genome-wide QV and QV* averages; 5) the -polish mode scores each variant, or variants within distance k and their combinations by the K* for polishing. Merfin is fully parallelized using OpenMP.

For manuscripts utilizing custom algorithms or software that are central to the research but not yet described in published literature, software must be made available to editors and reviewers. We strongly encourage code deposition in a community repository (e.g. GitHub). See the Nature Research [guidelines for submitting code & software](#) for further information.

Data

Policy information about [availability of data](#)

All manuscripts must include a [data availability statement](#). This statement should provide the following information, where applicable:

- Accession codes, unique identifiers, or web links for publicly available datasets
- A list of figures that have associated raw data
- A description of any restrictions on data availability

HG002 variant call data was downloaded from <https://data.nist.gov/od/id/mds2-2336> (SEX9X, NFT0L, 23O09, and QUE7Q). Sequencing data and assemblies for CHM13, HG002, and VGP genomes are available at <https://github.com/marbl/CHM13>, https://github.com/human-pangenomics/HG002_Data_Freeze_v1.0 and <https://vgp.github.io/>.

Source data used for generating all figures in this manuscript are available at <https://github.com/gf777/misc/tree/master/merfin/paper/figures>.

The K* tracks for HiFi and Illumina of the CHM13 are browsable in the associated UCSC browser (http://genome.ucsc.edu/cgi-bin/hgTracks?db=hub_2395475_t2t-chm13-v1.1). All variant calls used in the genotyping benchmarks, k-mer databases, fitted histogram tables and K* tracks are available to download at https://s3-us-west-2.amazonaws.com/human-pangenomics/index.html?prefix=publications/MERFIN_2021/ with a step-by-step guideline available at <https://github.com/aranghie/merfin/wiki/Best-practices-for-Merfin>. All data are publicly open for download with no restrictions.

Field-specific reporting

Please select the one below that is the best fit for your research. If you are not sure, read the appropriate sections before making your selection.

- Life sciences Behavioural & social sciences Ecological, evolutionary & environmental sciences

For a reference copy of the document with all sections, see [nature.com/documents/nr-reporting-summary-flat.pdf](https://www.nature.com/documents/nr-reporting-summary-flat.pdf)

Life sciences study design

All studies must disclose on these points even when the disclosure is negative.

Sample size	HG002 was selected for its well characterized known genotypes and toolkits available for benchmark. T2T-CHM13 was used for evaluation as this is the first and only complete human genome assembly to date. Three species (birds, reptiles, and fish) were chosen to demonstrate the utility of Merfin in non-human genomes.
Data exclusions	No data were excluded
Replication	All results can be reproduced using the version of softwares used. However, the tool we are presenting have been updated since then for improving computational performance and correcting unexpected flaws in the software. The latest version produces comparable or more accurate results however not changing the conclusion.
Randomization	Randomization was not performed because this study requires known truth sets for genotyping benchmark, a well characterized and complete genome assembly for evaluation, and published assemblies for comparing polishing outcomes.
Blinding	Blinding was not performed because this study requires known truth sets for genotyping benchmark, a well characterized and complete genome assembly for evaluation, and published assemblies for comparing polishing outcomes.

Reporting for specific materials, systems and methods

We require information from authors about some types of materials, experimental systems and methods used in many studies. Here, indicate whether each material, system or method listed is relevant to your study. If you are not sure if a list item applies to your research, read the appropriate section before selecting a response.

Materials & experimental systems

n/a	Involved in the study
<input checked="" type="checkbox"/>	<input type="checkbox"/> Antibodies
<input checked="" type="checkbox"/>	<input type="checkbox"/> Eukaryotic cell lines
<input checked="" type="checkbox"/>	<input type="checkbox"/> Palaeontology and archaeology
<input checked="" type="checkbox"/>	<input type="checkbox"/> Animals and other organisms
<input checked="" type="checkbox"/>	<input type="checkbox"/> Human research participants
<input checked="" type="checkbox"/>	<input type="checkbox"/> Clinical data
<input checked="" type="checkbox"/>	<input type="checkbox"/> Dual use research of concern

Methods

n/a	Involved in the study
<input checked="" type="checkbox"/>	<input type="checkbox"/> ChIP-seq
<input checked="" type="checkbox"/>	<input type="checkbox"/> Flow cytometry
<input checked="" type="checkbox"/>	<input type="checkbox"/> MRI-based neuroimaging